Atmospheric
Chemistry
and Physics

Influence of anthropogenic emissions on the composition of highly oxygenated organic molecules in Helsinki: a street canyon and urban background station comparison

Magdalena Okuljar[1], **Olga Garmash**[2,5], **Miska Olin**[2], **Joni Kalliokoski**[2], **Hilkka Timonen**[3], **Jarkko V. Niemi**[4], **Pauli Paasonen**[1], **Jenni Kontkanen**[1,6], **Yanjun Zhang**[1,7], **Heidi Hellén**[3], **Heino Kuuluvainen**[2], **Minna Aurela**[3], **Hanna E. Manninen**[4], **Mikko Sipilä**[1], **Topi Rönkkö**[2], **Tuukka Petäjä**[1], **Markku Kulmala**[1], **Miikka Dal Maso**[2], and **Mikael Ehn**[1]

[1]Institute of Atmospheric and Earth System Science/Physics, University of Helsinki, 00014, Helsinki, Finland
[2]Aerosol Physics Laboratory, Physics Unit, Tampere University, P.O. Box 692, 33014, Tampere, Finland
[3]Atmospheric Composition Research, Finnish Meteorological Institute, 00101, Helsinki, Finland
[4]Helsinki Region Environmental Services Authority, HSY, P.O. Box 100, 00066, Helsinki, Finland
[5]Department of Atmospheric Sciences, University of Washington, Seattle, WA, United States
[6]CSC – IT Center for Science Ltd., 02101, Espoo, Finland
[7]IRCELYON, University of Lyon, Université Claude Bernard Lyon 1, CNRS, 69626 Villeurbanne, France

Correspondence: Magdalena Okuljar (magdalena.okuljar@helsinki.fi)

Abstract. Condensable vapors, including highly oxygenated organic molecules (HOMs), govern secondary organic aerosol formation and thereby impact the quantity, composition, and properties (e.g., toxicity) of aerosol particles. These vapors are mainly formed in the atmosphere through the oxidation of volatile organic compounds (VOCs). Urban environments contain a variety of VOCs from both anthropogenic and biogenic sources, as well as other species, for instance nitrogen oxides (NO_x), that can greatly influence the formation pathways of condensable vapors like HOMs. During the last decade, our understanding of HOM composition and formation has increased dramatically, with most experiments performed in forests or in heavily polluted urban areas. However, studies on the main sources for condensable vapors and secondary organic aerosols (SOAs) in biogenically influenced urban areas, such as suburbs or small cities, have been limited. Here, we studied the HOM composition, measured with two nitrate-based chemical ionization mass spectrometers and analyzed using positive matrix factorization (PMF), during late spring at two locations in Helsinki, Finland. Comparing the measured concentrations at a street canyon site and a nearby urban background station, we found a strong influence of NO_x on the HOM formation at both stations, in agreement with previous studies conducted in urban areas. Even though both stations are dominated by anthropogenic VOCs, most of the identified condensable vapors originated from biogenic precursors. This implies that in Helsinki anthropogenic activities mainly influence HOM formation by the effect of NO_x on the biogenic VOC oxidation. At the urban background station, we found condensable vapors formed from two biogenic VOC groups (monoterpenes and sesquiterpenes), while at the street canyon, the only identified biogenic HOM precursor was monoterpenes. At the street canyon, we also observed oxidation products of aliphatic VOCs, which were not observed at the urban background station. The only factors that clearly correlate (temporally and composition-wise) between the two stations contained monoterpene-derived dimers. This suggests that HOM composition and formation mechanisms are strongly dependent on localized

emissions and the oxidative environment in these biogenically influenced urban areas, and they can also change considerably within distances of 1 km within the urban environment. This further suggests that studies should be careful when extrapolating single-point measurements in an urban setting to be representative of district or city scales.

1   Introduction

Urban environments can contain various anthropogenic and biogenic sources of volatile organic compounds (VOCs). Biogenic emissions come mostly from urban vegetation, for example, trees and bushes in parks and gardens, and may contain biogenic volatile organic compounds (BVOCs) such as isoprene, monoterpenes (MTs), or sesquiterpenes. The sources of anthropogenic emissions consist of traffic, cooking, industrial processes and the production of customer goods, and volatile chemical products (VCPs) (Li et al., 2022; Reimann and Lewis, 2007; Watson et al., 2001). Gas-phase compounds emitted from anthropogenic sources contain trace gases, including nitrogen oxides (NO_x), as well as anthropogenic volatile organic compounds (AVOCs), for example aromatic compounds or aliphatic hydrocarbons (Timonen et al., 2017; McDonald et al., 2018). In densely populated areas, VCPs can dominate AVOC concentrations, and compounds typically known as BVOCs (e.g., monoterpenes) are also emitted from anthropogenic sources, such as personal care products and cleaning agents (Gkatzelis et al., 2021; Li et al., 2022).

Under atmospheric conditions, VOCs can undergo oxidation to form condensable vapors (Pandis et al., 1992; Ehn et al., 2014). The most common ambient oxidants are ozone (O_3), hydroxyl radical (OH), and nitrate radical (NO_3) (Wayne, 2000). O_3 is a trace gas produced in the troposphere mostly by photolysis of NO_2 (Liu et al., 1980) and is present in the ambient air during the entire day. O_3 can oxidize only VOC containing at least one double or triple bound or, with a slower reaction rate, carbonyls (Bianchi et al., 2019). OH is a short-lived, highly reactive compound produced mostly by the photolysis of O_3 (Crutzen et al., 1999); thus OH is present in the atmosphere mainly during the daytime. NO_3 is a product of the reaction between O_3 and NO_2 and is rapidly destroyed by photolysis and reactions with NO during the daytime (Wayne et al., 1991). Both radicals can react with most closed-shell VOCs (Seinfeld and Pandis, 2016), but in the atmosphere, NO_3 reacts mostly with alkenes while OH reacts with almost all compounds, including aromatic hydrocarbons (Seinfeld and Pandis, 2016). Oxidation of VOCs almost always leads to peroxy radical (RO_2) intermediates, typically with lifetimes long enough to participate in bimolecular reactions, primarily with NO, HO_2, or other RO_2. The RO_2 may also undergo various unimolecular isomerizations, and both these and the bimolecular reactions can lead to either propagation or termination of the organic radical (Bianchi et al.,

2019). The structure of the final product depends on multiple factors, including the structure of the initial VOC and the "oxidative conditions", meaning available oxidants and the bimolecular reaction partners. The latter can be referred to as "terminators" when they terminate the oxidation process, and in some cases the product composition can tell us a lot about the oxidative conditions. For example, RO_2 termination by NO and oxidation by NO_3 can produce organic nitrogen compounds (ONCs) (Atkinson and Arey, 2003; Bianchi et al., 2019), while RO_2 termination by NO_2 can form relatively unstable peroxy nitrates. RO_2 cross-reactions are the only reactions that can form accretion products, ROOR, referred to here as "dimers" (Valiev et al., 2019).

RO_2 intermediates can also undergo autoxidation, where the RO_2 isomerizes through a hydrogen shift (H shift), creating an alkyl radical to which molecular oxygen can attach (Bianchi et al., 2019; Ehn et al., 2014; Crounse et al., 2013). In the end, a new, more oxidized RO_2 is formed, which can undergo either additional H shifts or bimolecular reactions, with both potentially terminating or propagating the oxidation (Bianchi et al., 2019) chain. In cases where the radical can undergo multiple autoxidation H shifts, the end product can reach oxidation levels high enough to be classified as highly oxygenated organic molecules (HOMs; Bianchi et al., 2019). The structure of a VOC strongly influences its propensity to undergo autoxidation and, consequently, the molar yield of HOMs. This results in very variable HOM yields, which can reach high values for different anthropogenic and biogenic compounds (Molteni et al., 2018; Bianchi et al., 2019; Garmash et al., 2020). Differences in the structural composition affect both the physical and the chemical properties of HOMs, with more oxidized products typically being less volatile (Kroll and Seinfeld, 2008). However, the exact functionalities are important, and, e.g., oxygen atoms in nitrate groups lower the volatility much less than if the oxygen were found in some other functional group (Kroll and Seinfeld, 2008). In general, the high oxygen content of HOMs makes them an important contributor to secondary organic aerosol (SOA) formation, influencing, e.g., air quality.

During the last decade, HOM formation from biogenic emissions has been extensively studied in forests (Ehn et al., 2014; Yan et al., 2016; Bianchi et al., 2017; Massoli et al., 2018) and in agricultural environments (Kürten et al., 2016). Recently, research showed that the oxidation of AVOCs can also noticeably contribute to the HOM population (Molteni et al., 2018; Garmash et al., 2020; Wang et al., 2021) and SOA formation (Timonen et al., 2017). Addition-

ally, NO_x can alter the HOM formation mechanism and influence SOA formation (Fry et al., 2014; Ng et al., 2017; Pullinen et al., 2020; Mutzel et al., 2021). Due to these findings, research on condensable vapors and their origin has focused more strongly on urban environments, especially very polluted ones, heavily influenced by anthropogenic emissions (Brean et al., 2019; Liu et al., 2021; Guo et al., 2022b; Nie et al., 2022; Yan et al., 2022). In very polluted environments, formation of condensable vapors is greatly impacted by NO_x (Brean et al., 2019; Liu et al., 2021; Guo et al., 2022b; Nie et al., 2022; Yan et al., 2022) and HOM composition is often dominated by AVOC precursors (Nie et al., 2022).

While the composition and formation of condensable vapors have been studied in the abovementioned forests and highly polluted locations, environments with considerable influence from both anthropogenic and biogenic emission sources have received much less attention. Such areas include urban environments with lots of green areas, for example suburbs or cities surrounded by large forests. A better understanding of such locations may also help to assess the impact on air quality of adding vegetation such as green roofs to already built-up areas. Helsinki is an example of a city with forests in close proximity, and Saarikoski et al. (2023) estimated that there, even at a street canyon site strongly affected by traffic emissions, BVOCs are the main contributor to oxidation products. While Saarikoski et al. (2023) measured only the composition of VOCs, and not their oxidation products, this finding makes us expect that the relative role of BVOCs is even higher for HOMs, as BVOCs typically have a higher propensity for autoxidation than AVOCs (Bianchi et al., 2019). Another important aspect to consider is the spatial representativeness of typical urban measurements. As cities are very inhomogeneous in terms of local emissions and the oxidative environment and HOMs are short-lived compounds, HOM studies in urban environments that were performed at one specific location may not be comparable to other nearby locations with different urban sub-environments.

Here we investigate the composition of condensable vapors at two nearby stations in Helsinki, which are differently influenced by anthropogenic emissions. The first station is located in a busy street canyon, while the second is in an urban background area, in a less densely built part of Helsinki, 150 m from the nearest busy road. We studied the composition of condensable vapors, mostly HOMs, at these sites using two nitrate-based chemical ionization mass spectrometers. To identify different HOM types from the mass spectra and connect them to different formation pathways, we applied positive matrix factorization (PMF) to separate covarying species. We compared the drivers of HOM formation between the two urban sub-environments and explored the roles of biogenic and anthropogenic emissions in HOM composition in order to understand how these can affect the air quality in urban environments with a strong biogenic influence.

2 Methods

We measured the composition of condensable vapors at two stations in Helsinki situated in contrasting environments: the Helsinki Region Environmental Services Authority (HSY) air quality station (60° 11′47.0″ N, 24°57′07.7″ E) and the Station for Measuring Ecosystem–Atmosphere Relations (SMEAR III; 60°12′10.4″ N, 24°57′40.2″ E) (Fig. 1). The HSY supersite is located at a street canyon, less than 1 m from the street of Mäkelänkatu (around 28 000 vehicles per weekday) (Kuuluvainen et al., 2018). The street canyon is 42 m wide, and the heights of buildings on both sides of the supersite are 19 and 16 m, leading to an average height-to-width ratio of 0.45 (Järvi et al., 2023). It contains a pavement and three lines of road for both directions separated by two tram lines and trees. SMEAR III is 900 m northeast of the HSY station and at 150 m distance from the closest busy road (the street Hämeentie). SMEAR III is classified as an urban background station (Järvi et al., 2009). The neighborhood of these stations was previously described in Okuljar et al. (2021). Here we refer to them as "street canyon" (later also "SC") and "urban background station" (later also abbreviated as "UB"), respectively.

The measurement campaign was conducted during 11 May 2018–3 June 2018 at the urban background station and 27 April 2018–24 May 2018 at the street canyon. The measurement period was during a change of season, and by 14 May 2018 the deciduous trees in the surrounding area had fully developed their leaves. To study the influence of traffic emissions, we analyzed separately the data measured during workdays as well as only during weekends and public holidays (1 and 10 May 2018). We refer to them as "workdays" and "weekends", respectively. As the nighttime concentrations are often influenced by the emission from the previous day, we separate these categories into 24 h periods starting at 04:00 local time (LT). The corresponding analysis of the size distribution of 1–1000 nm particles measured during the same time at both stations in Helsinki is presented by Okuljar et al. (2021).

The detailed meteorological description of the transport of pollutants at both stations with the emphasis on the mechanism affecting this transport at the street canyon is presented by Järvi et al. (2023). In summer the atmosphere is very stable during the nighttime and very unstable during the daytime at the urban background station. The meteorological conditions at the urban background station (Fig. 2) resemble those described by Järvi et al. (2023) for summer, which suggests limited vertical mixing of the atmosphere during the nighttime and a very well mixed lower atmosphere during the daytime during our measurement. At both stations, during the warm period the mechanical and thermal mixing is stronger than during cold periods, resulting in conditions more favorable for pollution dispersion (Järvi et al., 2023). At the street canyon, not only mean wind but also the turbulent mixing is important for the transport of pollutants. This may suggest
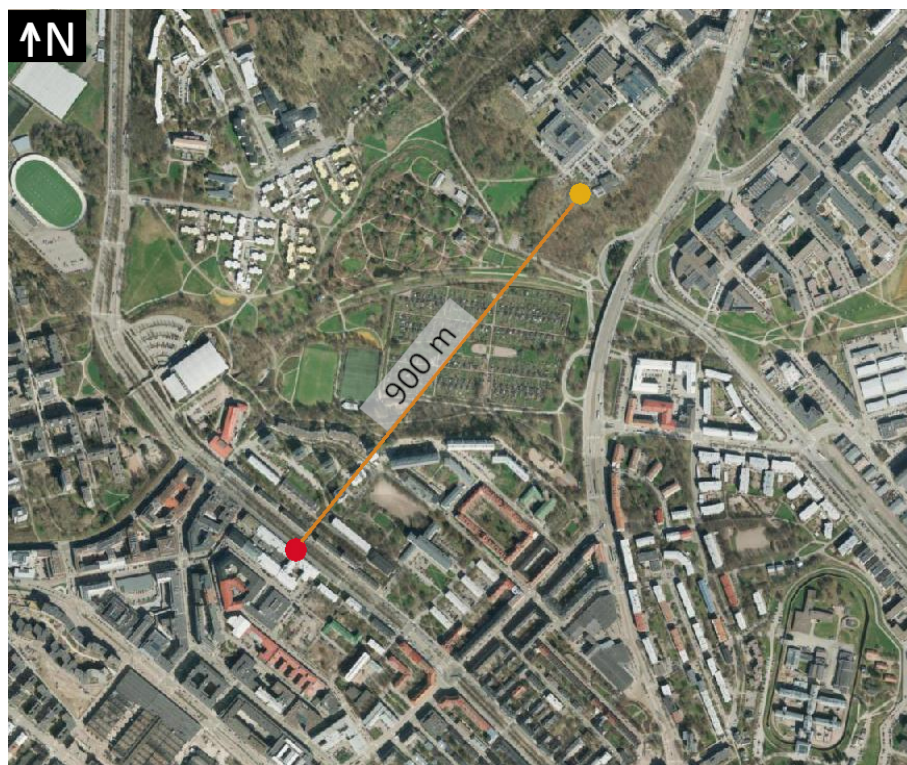
Figure 1. Orthophotograph of stations in the street canyon (red) and in an urban background environment (yellow) made on 7 May 2018. The photograph was provided by the City of Helsinki Map Service (CC BY 4.0).

that even though the air is not stagnant, the pollutants are not efficiently transported from the street canyon.

2.1 Condensable vapor measurements

The composition of condensable vapors was measured simultaneously at both stations by two nitrate-ion-based chemical ionization atmospheric pressure interface time-of-flight mass spectrometers (CI-APi-TOF) (Jokinen et al., 2012). Nitrate ions (NO_3^-), produced by interactions between soft X-ray and sheath air containing nitric acid (HNO_3), bind to the analyzed compound through hydrogen bonds or charge the analyte via proton transfer reactions. NO_3^- is primarily selective towards organic molecules containing at least two suitably positioned hydroxyl ($-OH$) or hydroperoxyl ($-OOH$) groups (Hyttinen et al., 2015) or compounds with higher gas-phase acidity than HNO_3. After the sample becomes ionized, the ions are focused in the APi module and ultimately separated in the TOF based on their mass-to-charge ratio (m/Q, reported in units of Th). The CI-APi-TOF and its working principles were described in detail by Jokinen et al. (2012). The resolving power of the mass spectrometer at both stations was approximately $3000–4000\,\mathrm{Th\,Th^{-1}}$ for signals with m/Q higher than 200 Th. The mass spectra were analyzed using the software package tofTools (Junninen et al., 2010).

In measured mass spectra, we observed multiple peaks at every m/Q. Performing high-resolution (HR) analysis requires us to fit closely set signals and could increase uncertainties in results. Therefore, most of our analysis is based on unit mass resolution (UMR) data, and we apply HR analysis at times when PMF indicated low interference with this factor, as described in Sect. 2.4. Additionally, we noted that condensable vapor measurement at the street canyon had lower transmission for higher m/Q than at the urban background station.

Here, we discuss quantitative changes in condensable vapors based on their measured signal in counts per second (cps) normalized by the cps of the reagent ions (NO_3^-, $HNO_3NO_3^-$, and $(HNO_3)_2NO_3^-$), using the unit ncps (normalized cps). The ambient concentrations can be estimated by using previously determined instrument-specific calibration coefficients for sulfuric acid (Okuljar et al., 2021) equal to $4\times10^9\,\mathrm{cm^{-3}}$ for the street canyon station and $7\times10^9\,\mathrm{cm^{-3}}$ for the urban background station. However, usage of these calibration coefficients determined for sulfuric acid to calculate HOM concentration comes with very large uncertainties, and we therefore concentrate on the comparison of ion signal strength.
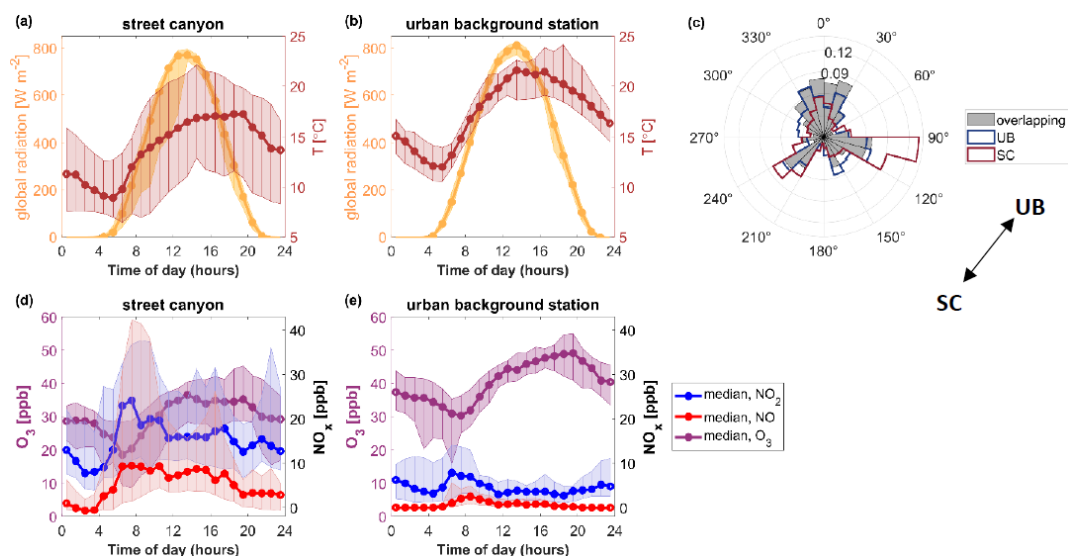
Figure 2. Diurnal variations in **(a, b)** global radiation and ambient temperature, and **(d, e)** NO, NO_2, and O_3 concentrations at the street canyon **(a, d)** and urban background station **(b, e)**. The median diurnal variations are shown as solid lines with markers; the 25th to 75th percentile ranges are presented as shaded areas. Time is local. Panel **(c)** shows a wind rose for the overlapping time at both stations as well as an outline of a wind rose for the period when data were collected from the street canyon (SC, dark red) and the urban background station (UB, dark blue). The arrow in panel **(c)** shows the direction of the urban background station (UB) in relation to the street canyon (SC). Presented data contain both workdays and weekends.

2.2 VOC measurements

VOC concentrations were measured at the street canyon with an offline method in which ambient samples were first collected on a Tenax TA Carbopack B sorbent tube and later analyzed by thermal desorption gas chromatography coupled with mass spectrometry (TD-GC-MS). We measured VOC concentrations during the period 15–25 May 2018 with 4 h time resolution. A total of 13 analytes were classified as AVOCs – benzene, toluene, ethylbenzene, p-/m-xylene, styrene, o-xylene, propylbenzene, 3-ethyltoluene, 4-ethyltoluene, 1,3,5-trimethylbenzene, 2-ethyltoluene, 1,2,4-trimethylbenzene, and 1,2,3-trimethylbenzene – and 15 as BVOCs – monoterpenoids (α-pinene, camphene, β-pinene, Δ3-carene, p-cymene, 1,8-cineol, limonene, terpinolene), terpene alcohol (linalool), an oxidation product of β-pinene (nopinone), bornyl acetate, and sesquiterpenes (longicyclene, isolongifolene, β-caryophyllene, and α-farnesene). A more detailed description of the method can be found, e.g., in Helin et al. (2020).

2.3 Other instrumentation

CO_2, NO, NO_2, SO_2 as well as meteorological variables were measured at both stations. Table S1 in the Supplement contains information about measurements of additional variables used in this paper.

2.4 Positive matrix factorization

Collected datasets from the measurement of condensable vapors at both stations consist of an enormous amount of information, and it is challenging to filter data that contain relevant information for analysis of HOM formation. As both stations are located in a city, the composition of condensable vapors is dependent on different types of VOC sources as well as chemical and meteorological conditions. To extract relevant information, separate different pathways of HOM formation, and find processes affecting condensable vapor composition at both stations, we applied positive matrix factorization (PMF) (Paatero, 1997; Paatero and Tapper, 1994; Paatero and Hopke, 2003). PMF is a multivariate factor analysis model which has been widely used on aerosol mass spectrometry data (Ng et al., 2011; Zhang et al., 2011; Chen et al., 2022) and more recently on ambient gas-phase chemical ionization mass spectrometry data (Yan et al., 2016; Massoli et al., 2018; Zhang et al., 2019; Liu et al., 2021; Nie et al., 2022).

We performed PMF analysis on three different m/Q ranges from UMR data at both stations: 200–350, 350–500, and 500–650 Th. In this paper, we will refer to these ranges as ranges 1, 2, and 3, respectively. The loss rate of HOMs due to condensation is roughly a function of their mass (Peräkylä et al., 2020); thus, analyzing mass spectra in ranges allows us to group HOMs with similar loss rates and focus specifically on separating the HOM sources (Zhang et al., 2020). Additionally, when an m/Q range has lower signal than other ranges, it will only have a minor weight on the PMF solution

and relevant information may be lost (Zhang et al., 2020). Using m/Q ranges for PMF analysis is important especially at the street canyon as it may partly counteract the loss of information due to lower transmission for higher m/Q. The focus of our analysis is on compounds in a range of 200 to 650 Th as in this reach we can find the majority of the condensable vapors containing C_{5-20}. Smaller m/Q values are unlikely to condense, while larger m/Q values had very low, or even negligible, signals. We prepared data and error matrices with 30 min time resolution, separately for each range at each station according to the methods described by Yan et al. (2016). To conduct PMF analysis, we used the Igor-based interface Source Finder (SoFi, version 6.D) (Canonaco et al., 2013) and ME-2 solver (Paatero, 1999). Detailed information about data preparation and validation of PMF solutions can be found in Sect. S1.

To describe the chemical composition of ions in obtained factors, we determined the times for each factor when that factor had the highest relative contribution to the total signal and then fit peaks to the HR data to identify the key compounds. Choosing times when the analyte is dominant across all factors in the same m/Q range and at the same site is necessary to ensure that the identified compound is correctly assigned to the factor. In this paper, we performed a more detailed interpretation only of chosen factors from each station, which we refer to further on as "selected factors". A factor was chosen for further interpretation only when we could reasonably identify ions in it and relate it to a real atmospheric source, i.e., not impurities. We refer to other factors as "not selected factors". Examples of each type will be given later to better clarify this selection process.

2.5 Limitation of data for interpretation

The are several limitations for interpreting the data. At the street canyon, a low signal is observed for higher m/Q. That leads to a low signal-to-noise ratio (S/N) for HOMs measured in ranges 2 and 3 and in some cases makes it impossible to identify the compounds. As a result of a fast decrease in measured signal with an increase in m/Q, at the street canyon, over 90 % of the signal of 200–650 Th is located in range 1. This could be caused by a lower transmission for high m/Q of the CI-APi-TOF measurement at that station. Transmission is a result of voltage settings used with CI-APi-TOF, which are optimized for each instrument separately. We could not correct our data for transmission. Zha et al. (2018) showed that the ratio of the signal for the same sampled air measured by two CI-APi-TOF instruments can change drastically with an increase in m/Q due to the difference in the transmission between instruments. Thus, the highest uncertainty caused by inconsistent transmission between two instruments is observed in range 3. Nevertheless, this uncertainty does not influence identification of peaks that have sufficient S/N.

Due to the chemical complexity of the samples, we cannot achieve high accuracy of mass calibration on some of the measured days. This is the reason why we have performed PMF analysis on UMR data. Limitations of peak identification due to the resolution of the mass spectrometer and the presence of multiple overlapping peaks also hinder the identification of some ions, and hence we are only confident to report the dominant ions in each factor. We are not able to report key compounds for factors that have a minor contribution to their m/Q range or have too many similar peaks with other factors, as we cannot unambiguously assign identified compounds to these specific factors.

Lastly, we need to keep in mind that chemical ionization with NO_3^- is very selective, mostly towards highly functionalized compounds. Overall, this ionization method is optimal for the detection of HOMs; however, it limits observations of other oxidation products.

3 Results and discussion

We start this section by providing a short overview of the meteorological conditions during the campaign. In Sect. 3.2, we present our main findings, starting from the PMF results and the subsequent interpretations of important formation pathways of condensable vapors at the two measurement sites. In the last part of this section, we discuss the potential implications of our findings for the air quality in Helsinki.

Concerning notations, we focus our study on HOMs, but we also detect abundant organic compounds which contain fewer than six oxygen atoms, which are not classified as HOMs. Thus, we often use a broader term, "condensable vapors", when discussing observed products more broadly. In addition, we observe monomeric (mostly C_9–C_{10}) and dimeric (mostly C_{19}–C_{20}) oxidation products of MTs, which we refer to as "MT-derived monomers" and "MT-derived dimers", respectively. For simplicity, we call factors containing monomeric oxidation products of MTs "MT monomers", while factors referred to as "MT dimers" contain dimeric oxidation products of MTs.

3.1 Overview of meteorological and trace gas conditions in Helsinki

Atmospheric conditions, for example local emissions and the oxidative environment, influence HOM formation pathways. To understand HOM formation mechanisms and their differences between studied sites, we first investigated meteorological and chemical conditions at both stations. Figure 2 presents diurnal variations in measured variables that can influence HOM formation pathways: global radiation; ambient temperature (T); and concentrations of O_3, NO, and NO_2 as well as the wind direction measured during this campaign. As mentioned earlier, the measurement periods overlapped but were not identical between the two stations. Therefore, differences in campaign averages between sites are partly driven

by differences in location and partly by differences in time. The differences in meteorological parameters (ambient temperature, global radiation, wind direction) are driven mostly by changes in the measurement period (Figs. 2, S2), while the trace gases (NO, NO$_2$, O$_3$) also vary largely during overlapping times of measurements (11–24 May 2018) (Fig. S2).

Diurnal variation in global radiation is similar between the two stations (Fig. 2a, b), though with slightly more cloudy periods at the street canyon. Global radiation initiates photolysis reactions and, as a result, enhances the formation of OH and O$_3$ as well as the decomposition of NO$_3$. During the overlapping time of measurements, the urban background station was more likely to be the downwind station; however the wind was mostly coming from the north (Fig. 2c), meaning that neither station would receive emissions from the other. Median temperatures varied between 12.0 and 21.6 °C at the urban background site and between 8.9 and 17.3 °C in the street canyon. Higher temperature at the urban background station can be explained by the difference in measurement periods as the measurements started 2 weeks later than in the street canyon. During the period when measurements overlapped, the median temperature is very similar between stations, reaching almost 22 °C during the daytime and dropping to 12–13.4 °C during the nighttime (Fig. S2). The increase in temperature typically accelerates molecular reaction rates as well as enhances BVOC emissions and evaporation rates. It can also affect HOM yields (Quéléver et al., 2019).

At the urban background station, NO has a maximum between 08:00 and 09:00 LT (2.5 ppb) and it is negligible during the nighttime. In contrast, at the street canyon, the median NO concentration was below the detection limit between 01:00 and 03:00 LT, after which it rapidly increased, leveling off at 07:00 LT and staying elevated (ca. 9 ppb) throughout the day until 17:00 LT. That means NO can affect oxidation reactions more at the street canyon site, even during much of the night, when it stays at 4 ppb until the early morning. In the context of VOC oxidation, the presence of NO likely causes the termination of the oxidation. In the absence of NO, termination reactions with RO$_2$ become more favorable. NO$_2$ and NO (Fig. 2c, d) concentrations are up to 5 and 23 times higher at the street canyon than at the urban background station, respectively. At the urban background site, O$_3$ reaches a minimum median concentration at 07:00 LT (30.3 ppb) and maximum at 19:00 LT (49.1 ppb). At the street canyon, the corresponding values are 18.5 ppb at 06:00 LT and 36.5 ppb at 13:00 LT. During overlapping times between the sites, median O$_3$ concentration stays 5–25 ppb lower at the street canyon than at the urban background station (Fig. S2). This could be partly associated with higher NO concentration in the street canyon as NO reacts with O$_3$. O$_3$ remains relevant for VOC oxidation throughout the day. O$_3$ and NO$_2$ concentrations affect the production of NO$_3$ and thus its concentration.

3.2 Characterization of PMF factors

In this subsection, we examine the HOM composition and formation at both stations by investigating PMF factors in all three m/Q ranges (200–350, 350–500, 500–650 Th); we focus our analysis on selected factors, their time series (Figs. S3–S4), and diurnal variations (Figs. 3–4) as well as mass spectra (Figs. S5–S6). We refer to PMF factors as SCX-Y or UBX-Y, where SC is the street canyon, UB is the urban background station, X is the analyzed m/Q range (either 1, 2, or 3), and Y is the identifying number of the factor in that range. The factors also appear together with a descriptive name. As an example, "UB3-2: MT dimers" refers to the second PMF factor identified in mass range 3 at the urban background site and was found to mainly contain ions related to monoterpene-derived dimers. To understand the chemical composition of factors, we identify their key compounds with HR data (Table S2) as described in Sect. 2.5. All key compounds are detected as clusters with NO$_3^-$ or HNO$_3$NO$_3^-$, and this is how we report them in Table S2 and on the mass spectra (Figs. S5–S6 and S9–S10); however, for clarity of the interpretation in this subsection, we write their chemical structures without the nitrate adducts.

In this subsection, we summarize the key characteristics and give an interpretation of factors. A more detail description of the PMF analysis can be found in the Supplement (Sect. S2, "PMF inputs and validation"; Sect. S4, "Factor interpretation"). Only selected factors are described here, while characteristics of not selected factors are presented and described in the Supplement (Sect. S4, Figs. S9–S10, Table S3). Several reasons motivated us not to include not selected factors for detailed discussion in the main text. For example, a factor was not selected if it was contamination or an artifact (e.g., containing mainly water clusters isotopes) or if we were not confident in the meaningful separation of this factor by the PMF method (this was the case for the whole of range 1 at the street canyon, as described below). Overall, we selected 5 out of 13 factors from the street canyon and 10 out of 14 factors from the urban background station. These selected factors explain 34 %, 100 %, and 100 % of the observed signal in ranges 1–3 at the urban background station and 0 %, 64 %, and 61 % of the observed signal in ranges 1–3 at the street canyon, respectively (Table 1, Figs. S7–S8).

3.2.1 Street canyon

Here, we very briefly describe factors observed at the street canyon site in each m/Q range. The main examination of the factors is given in Sect. 3.2.3, where we also discuss them in relation to factors observed at the urban background station. As already indicated above, PMF solutions for range 1 at the street canyon were inconclusive, and therefore all factors from this range are classified as not selected. The main reason for this is that all factors had very similar temporal trends, mainly correlating with temperature. This may be a
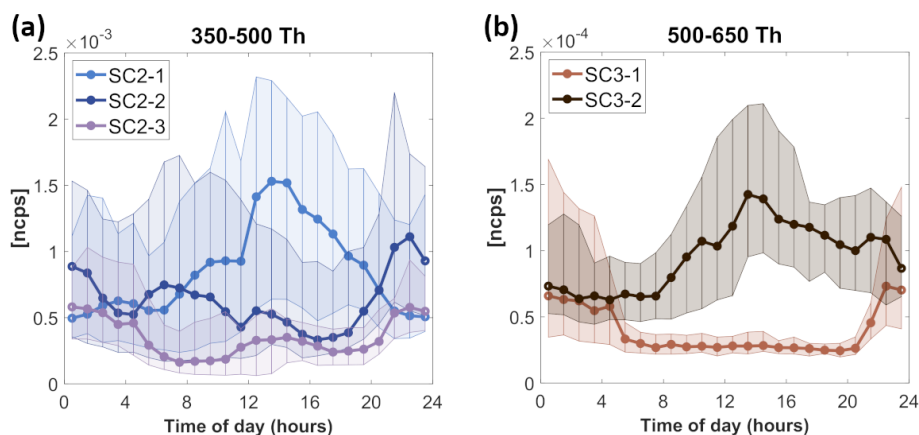
Figure 3. The diurnal variation in PMF factors fractions at the street canyon (SC). PMF factors are labeled as SCX-Y, where X stands for the analyzed m/Q range (2 or 3) and Y is the identifying number of the factor in that range. The median diurnal variation is shown as a solid line with markers; the 25th to 75th percentile ranges are presented as shaded areas. The y axis in ncps indicates the measured signal in normalized counts per second. Time is local.
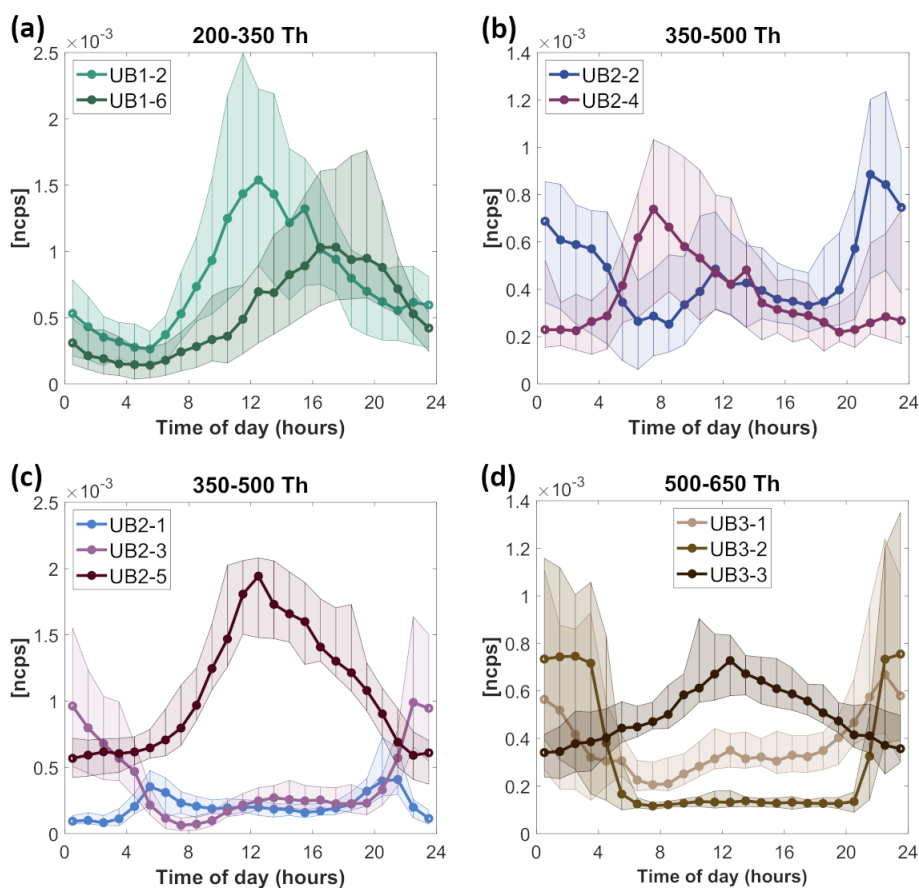

Figure 4. The diurnal variation in PMF factors at the urban background station (UB). PMF factors are labeled as UBX-Y, where X stands for the analyzed m/Q range (1, 2, or 3) and Y is the identifying number of the factor in that range. The median diurnal variation is shown as a solid line with markers; the 25th and 75th percentile ranges are presented as shaded areas. The y axis in ncps indicates the measured signal in normalized counts per second. Time is local.

Table 1. Suggested characterization of selected factors at both stations. Detailed factor interpretation is described in Sect. S3. The importance of the various species described in this table was assessed based on either factor time series (superscript TS), factor mass spectra (superscript MS), or both (superscript B), as indicated in the "Factor" column. The "Precursor" column describes which types of molecules we expect to act as precursors to the observed signals, separating (when possible) between AVOCs and BVOCs. The "Oxidant" and "Terminator" columns depict our estimates for the most likely species involved in the oxidation process ("m", as in "maybe", is used if we were unable to exclude or confirm the participation of the species). If the "yes" or "no" is marked in bold font, it means that we found a particularly clear influence of that species for that factor. The "Diurnal peak time" column shows the hour when the factor had its highest concentration, and "Fraction" depicts the percentage of signal (of the given sub-range or the total analyzed m/Q range) that the factor contributed to.

Range [Th]	Factor	Precursor	Oxidant			Terminator			Diurnal	Fraction [%] within	
			OH	NO$_3$	O$_3$	NO	RO$_2$	HO$_2$	peak time	200–650	sub-range
Street canyon											
350–500	SC2-1^{TS}	BVOCs	m	no	m	yes	no	m	13	2.2	27.2
	SC2-2^{TS}	VOCs	no	**yes**	m	m	no	m	22	2.0	24.8
	SC2-3^{TS}	BVOCs	no	**yes**	no	no	m	m	0	0.9	11.5
500–650	SC3-1^{B}	BVOCs	no	yes	no	**no**	yes	no	22	0.1	19.3
	SC3-2^{MS}	VOCs, noise, F impurities	yes	no	m	yes	no	m	13	0.2	41.6
Urban background station											
200–350	UB1-2^{MS}	AVOCs	**yes**	no	no	yes	no	m	12	8.9	16.1
	UB1-6^{TS}	VOCs	m	no	m	yes	no	m	17	7.4	17.8
350–500	UB2-1^{TS}	BVOCs	no	**yes**	no	yes	no	m	21	2.6	8.6
	UB2-2^{TS}	BVOCs	no	yes	m	**no**	m	m	21	5.4	18.0
	UB2-3^{MS}	BVOCs	no	yes	m	**no**	no	m	22	5.1	17.0
	UB2-4^{TS}	BVOCs	m	no	m	**yes**	no	m	7	4.9	16.5
	UB2-5^{MS}	VOCs, noise	**yes**	no	m	yes	no	m	12	12.0	39.9
500–650	UB3-1^{B}	BVOCs	no	yes	m	**no**	no	m	22	4.9	34.3
	UB3-2^{B}	BVOCs	no	yes	m	**no**	yes	no	23	3.6	25.4
	UB3-3^{MS}	VOCs, noise	**yes**	no	no	yes	no	m	12	5.6	40.3

result of most observed molecules being semi-volatile, and increased temperatures lead to increased evaporation of these molecules. In any case, as PMF relies on temporal variability to separate factors, too much co-variance makes PMF less reliable. Nevertheless, we believe there was also some useful information in this range and will briefly discuss SC1-1: nitrophenol 1, SC1-2: MT monomers 3, and SC1-5: nitrophenol & aliphatic in this section.

Range 1, 200–350 Th (factors selected: 0/5)

In range 1, all factors are affected by changes in ambient temperature (Figs. S9 and S13). Factors in range 1 have a daytime peak, and nearly all of them could have been oxidized by OH or O$_3$ (Fig. S9, Table S3). Most of these factors are likely formed from AVOCs and contain nitrophenol ($C_6H_5O_3N$) as well as other N-containing aromatics, such as nitrocresol. Nitrophenol can be directly emitted from combustion or formed from benzene and phenol oxidation. The presence of nitrophenol in many factors can be explained by an abundance of benzene at the street canyon as it is the third most abundant VOC measured at the street canyon site (Fig. S11).

Range 2, 350–500 Th (factors selected: 3/5)

In range 2, all selected factors respond to the changes in the ambient temperature (Figs. S3 and S13), especially factor SC2-1, which contains monomeric oxidation products of MTs (MT-derived monomers) with nitrate functionalities ($C_{10}H_{16}O_{8-10}N_{0-2}$ and/or $C_9H_{14,16}O_{9-10}N_2$). Factors SC2-2 and SC2-3 are highest during the night, but they also have local maxima during the day, which suggests that competing processes influence the formation of these factors and thus their diurnal pattern. SC2-3 may be inhibited by NO, as it decreases when NO reaches its daily maximum (Fig. 3d). SC2-3 consists of MT-derived monomers ($C_{10}H_{16}O_{10-11}N_2$ and $C_{10}H_{16}O_{10}$), while SC2-2 is dominated by one single compound: $C_{10}H_{16}O_9N_2$.

Range 3, 500–650 Th (factors selected: 2/3)

Range 3 contains one daytime and one nighttime factor. SC3-1 is an MT-derived dimer factor produced via oxidation by NO$_3$ and is present during the night, when NO concentrations are low enough to allow RO$_2$ termination via RO$_2$ cross-reactions. The key compounds detected in SC3-1 come from

one oxidation chain: $C_{20}H_{32}O_{11-15}N_2$. SC3-2 is a daytime factor containing HOMs oxidized by OH ($C_{19}H_{22,24}O_{10}N_2$). SC3-2 also has some signal from instrumental impurities containing fluorine (F impurities) and undefined noise peaks.

3.2.2 Urban background station

Similarly to the previous sub-subsection, we describe briefly factors observed in all ranges at the urban background station. A discussion about these factors follows in Sect. 3.2.3, in which we compare factors found at both sites in Helsinki.

Range 1, 200–350 Th (factors selected: 2/6)

Selected factors in range 1 contain daytime factors, from which UB1-6 is the factor correlating the best with the ambient temperature (Figs. S4 and S14). The time series of UB1-6 correlates with O_3 (Figs. 4a, S14), and it contains key compounds with C_{7-8} atoms. These formulas have been detected earlier as products of MT oxidation in chamber studies (Yan et al., 2020) and in ambient measurement (Liu et al., 2021); however, they have also been identified as oxidation products of aromatic VOCs (Guo et al., 2022b). Since the CI-APi-TOF does not provide information about molecular structure, we cannot unambiguously determine the origin of this factor. In contrast to UB1-6, the UB1-2 factor contains nitrophenol and likely originates from AVOCs. The diurnal variation in UB1-2 resembles the one expected for OH (Saarikoski et al., 2023). Both UB1-2 and UB1-6 contain ONCs, and their oxidation was likely terminated by NO or NO_2.

Range 2, 350–500 Th (factors selected: 5/5)

Range 2 contains various daytime and nighttime factors (Fig. 4). Factor UB2-1 reaches the highest concentrations at 05:00 and 22:00 LT, which corresponds to the time of sunrise and sunset during our measurement period. As this factor consists of MT-derived ONCs, possibly with at least two N atoms ($C_9H_{14}O_{9,11}N_2$ or $C_{10}H_{16}O_{9,11}N$ and $C_{10}H_{17}O_{12}N_3$), we can speculate that they are formed from NO_3 oxidation of MTs and terminated by NO. Chamber experiments have shown that formation of condensable vapors through NO_3 oxidation and NO termination is a possible formation mechanism during NO_x-influenced oxidation of monoterpenes (Yan et al., 2020; Nie et al., 2023). It is typically assumed that NO_3 and NO would not co-exist in the atmosphere. However, in urban areas NO concentration is not negligible during the night, and this pathway was previously suggested as a possible mechanism of ONC formation in Beijing (Guo et al., 2022b). The simultaneous presence of NO_3 and NO when photolysis is just high enough to form NO but not fully deplete NO_3 is a plausible explanation for the diurnal pattern of UB2-1.

UB2-2 and UB2-3 are both nighttime factors oxidized mainly by NO_3 and inhibited by NO during the daytime. UB2-2 contains MT-derived monomers and correlates with the MT-derived dimer factor (UB3-2). Following the diurnal cycle in Fig. 4b, it can be observed that when the concentration of UB2-2 decreases, the concentration of the daytime MT-derived monomer factor, UB2-4, increases. Even though UB2-2 and UB2-4 both contain key compounds with C_{9-10}, the molecular formulas are slightly different. Specifically, in UB2-2 key compounds contain mainly one or three N atoms while in UB2-4 they have mostly zero or two N atoms (Table S2). UB2-2 and UB2-4 could thus be formed from competing HOM formation pathways from the same VOCs.

In contrast to other factors, UB2-3 consists of HOMs with a composition of $C_{15}H_{23}O_{8,10,12-13}N$, based on which we conclude that this factor is formed from sesquiterpenes ($C_{15}H_{24}$; Richters et al., 2016). UB2-3 correlates very well with a corresponding sesquiterpene factor from range 3, UB3-1 ($R = 0.93$) (Fig. S12). The last factor UB2-5 is a daytime factor which at noon corresponds to more than 50 % of the measured signal (Fig. S8). It contains C_{10} compounds ($C_{10}H_{11}O_9N$ and $C_{10}H_{16}O_9N_2$), and it is most likely that UB2-5 is formed in OH oxidation.

Range 3, 500–650 Th (factors selected: 3/3)

Range 3 at the UB site contains two nighttime factors: the sesquiterpene-derived UB3-1 factor ($C_{15}H_{23}O_{10-13}N$ and $C_{15}H_{23}O_{14-16}N$ (or $C_{15}H_{24}O_{13-16}N_2$)) and MT-derived dimer UB3-2 factor (mostly containing C_{20} compounds, for example $C_{20}H_{32}O_{13-16}N_2$). Both factors consist of ONCs, products of NO_3 oxidation of BVOCs, and are inhibited by NO and absent during the day as a result. UB3-3 is the only daytime factor (Fig. 4d) in range 3, and it consists of OH-oxidized HOMs, F impurities, and noise.

3.2.3 Factor interpretation and comparison between urban background and street canyon sites

Tables 1 and S3 present the most plausible interpretation of selected and not selected factors, respectively. For each factor, we propose VOC precursors, oxidants, and terminators which were most likely to influence the formation of species in this factor. We also specify an hour of the day when the factor's signal reached its maximum as well as the contribution of this factor to the total signal both within its own m/Q sub-range and within the full analyzed range (200–650 Th). See Table 1 caption for a more detailed description of how to read the table. The findings and implications are discussed below. While discussing time series correlations between factors from both stations, it is important to keep in mind that they cannot be ideal. We estimated that the highest correlation between stations for condensable vapors is approx. 0.88, which is a correlation between concentrations of

a compound that is mostly produced in the same pathway on both sites: sulfuric acid (SA) (Fig. S15).

The total concentration of AVOCs is much higher than BVOCs at both stations (shown for the street canyon in Fig. S11); however, most of the selected factors are more likely to have a biogenic origin, primarily based on the identified peaks in the mass spectra (Table 1, Sect. S4). Our result is in agreement with the earlier study by Saarikoski et al. (2023), which concluded that, despite dominant AVOC concentrations at the street canyon site, BVOCs are estimated to be the main source of oxidized products due to their higher reactivities. MTs are the only type of biogenic precursors identified at the street canyon, while at the urban background station we find oxidation products of both MTs and sesquiterpenes. This is likely due to the difference in proximity of trees and vegetation to the stations as none of the measured sesquiterpenes exceeded 0.2 % of measured total BVOC concentrations at the street canyon. All key compounds detected in MT-derived factors were previously reported in studies investigating the influence of NO_x on HOM formation from MT precursors (Pullinen et al., 2020; Yan et al., 2020; Shen et al., 2021; Dam et al., 2022; Guo et al., 2022a). MTs can also be emitted from anthropogenic sources, for instance in the form of VCPs (Gkatzelis et al., 2021; Li et al., 2022). VCPs are known to be very important emitters (Karl et al., 2018); however, based on our results, it seems that the concentrations of biogenic terpenes are the main contributor to the formation of organic condensable vapors. This is because the population density of Helsinki is low enough for the VCP-emitted MT signature to be likely lost among the abundant biogenic MT signals. Additionally, it is probable that the biogenic terpenes are to a large extent transported into Helsinki from more rural areas, but emissions of biogenic terpenes within Helsinki can also be important, as has been shown to be the case in various cities (Kota et al., 2014; Kaltsonoudis et al., 2016; Rantala et al., 2016; Kaser et al., 2022). This is in agreement with α-pinene being the most abundant BVOC and a common VCP-emitted MTs, limonene (Coggon et al., 2021), being very low (<5 % of BVOC concentration).

We observed only a few PMF factors that we expect to originate from AVOC oxidation, and for both stations AVOC factors are detected only for the smallest m/Q sub-range, 200–350 Th (Tables 1, S3). None of the factors had diurnal variations resembling traffic emissions at these sites (Olin et al., 2020; Okuljar et al., 2021). Even though concentrations of some factors differed between weekends and workdays, the diurnal behavior of factors was very similar (Figs. S16–S17). This suggests that the local emissions from traffic at these sites did not oxidize fast enough, and with high enough yields of detectable compounds, to considerably contribute to our measured signals. This is in line with conclusions presented by Brean et al. (2019) and Saarikoski et al. (2023). As precursor VOC concentrations are also affected by the mixing layer height (MLH), this effect may also impact HOM formation. However, VOCs are only one of the components

that affect HOM formation; the effect of the MLH on HOMs observed in this study is expected to be small.

Between the two stations, there are only a few factors with similar key compounds (Table S2). SC3-1: MT dimers has key compounds that partly correspond with UB3-2: MT dimers. They both contain $C_{20}H_{32}O_xN_2$ compounds, where x is 11–15 for SC and 13–16 for UB. UB3-2: MT dimers also contains other types of dimers which are not usually present in SC3-1: MT dimers. These slight differences between stations may be caused by the small difference in the concentration of oxidants or the concentration or type of MT. The non-negligible concentration of NO during the nighttime at SC may also impact the dimer formation there. Nevertheless, these factors are very similar and form through similar pathways (Table 1) – oxidation of MTs mostly by NO_3 and termination through RO_2 cross-reactions, leading also to correlating time series ($R = 0.77$, Figs. 5 and S12). The $RO_2 + RO_2$ reactions forming the MT-derived dimers will inevitably also form monomers as the dimer yield is never 100 %. However, monomers can also form through all other RO_2 termination channels, making them much more heterogeneous than the dimers. The time evolution of some MT-derived monomer factor time series (SC2-3: MT monomers 2 and UB2-2: MT monomers 2) correlates with the corresponding dimer factors ($R = 0.7$ and $R = 0.67$, respectively) as well as with each other ($R = 0.57$). While both factors are dominated by C_{10} compounds, their detailed mass spectra have significant differences (Figs. S5 and S6): UB2-2: MT monomers 2 contains mainly ONCs with one N atom, while SC2-3: MT monomers 2 has more compounds with two N atoms (Table S2). This may indicate that there is enough NO available to terminate some fraction of the RO_2 yet without totally shutting down the $RO_2 + RO_2$ channel.

Another pair of factors showing similarities between the stations is SC2-2: 370+433 and UB2-4: MT monomers 3 (Fig. 5). Both factors are driven mostly by one compound ($C_{10}H_{16}O_9N_2$), which has been detected as two clusters $C_{10}H_{16}O_9N_2 \cdot NO_3^-$ (370 Th) and $C_{10}H_{16}O_9N_2 \cdot HNO_3 \cdot NO_3^-$ (433 Th) in our instrument (determined by correlation analysis). The high time series correlation ($R = 0.75$) suggests that molecules in these factors are formed via very similar pathways between the sites. Potentially, the formation pathways are identical, but the importance of some competing pathways differs between the sites. Overall, the lack of stronger resemblance between these nearby sites suggests that even if HOMs have the same VOC precursors, the environmental conditions regulate the relative importance between different oxidation pathways.

While differences in emissions and oxidation reactions will lead to diverse mass spectra, the time series are also expected to vary between the sites as the wind direction changes. For example, the street canyon site will likely be impacted by the street in different ways if the wind direction is from the street or towards the street. A clearly longer campaign than ours would be needed to identify the detailed
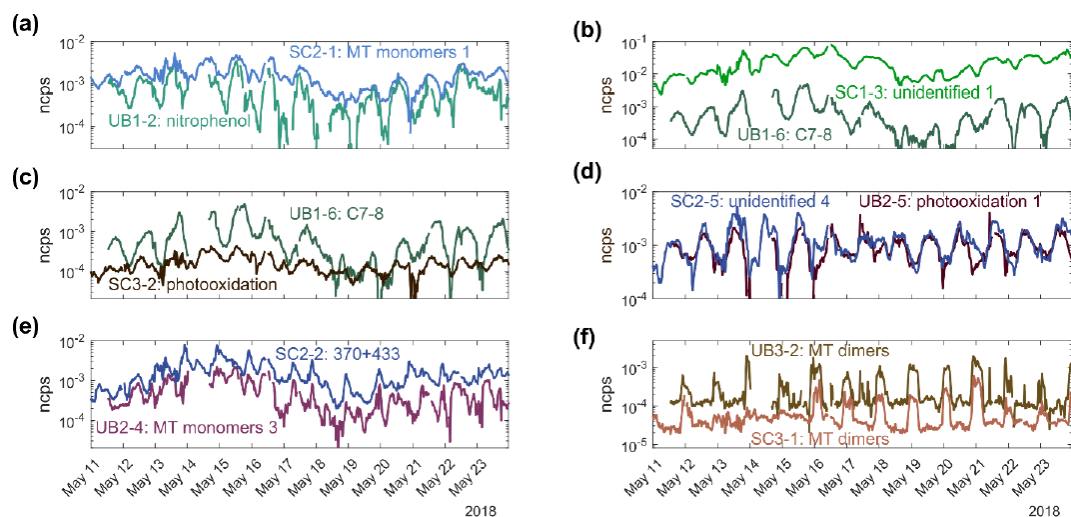
Figure 5. Time series of PMF factors with a Pearson correlation coefficient higher than 0.7 (Fig. S12) between the street canyon (SC) and the urban background station (UB) for a common measurement time. PMF factors are labeled as SCX-Y or UBX-Y, where X stands for the analyzed m/Q range (1, 2, or 3) and Y is the identifying number of the factor in that range.

impacts from different wind directions. However, analysis of the average diurnal variation can help us understand the roles of different oxidation conditions if the impact of varying wind directions diminishes for a longer average. Most factors at both stations can be characterized by one of a few types of diurnal patterns. Factors with a daytime diurnal variation reaching their maximum concentration at noon or during the afternoon resemble diurnal variation in OH and O_3, respectively. However, temperature also peaks in the afternoon and can lead to both higher BVOC emissions and evaporation of semi-volatile species from aerosols or surfaces, convoluting the effect of the oxidants on the observed HOMs. Factors with noon or afternoon maxima are mostly found in range 1 at both sites. As range 1 mostly contains species thought to be semi-volatile (Peräkylä et al., 2020), it is possible that much of the observed variation is indeed due to the higher temperature causing increased partitioning of these compounds into the gas phase. Nevertheless, OH and O_3 are likely involved as well, and given that the vast majority of signals are ONCs, RO_2 termination by NO is to be expected for most species. The opposite can be said for nighttime factors, which are likely inhibited in the daytime by NO, as their formation involves RO_2 termination via other pathways. This becomes especially visible for HOMs terminated via $RO_2 + RO_2$ reactions (Ehn et al., 2014; Yan et al., 2016), which are mainly present in range 3. In this range, the volatilities are overwhelmingly low or extremely low, meaning that ambient temperature changes will not impact their ability to condense irreversibly to aerosols, thus also making their temporal behavior easier to interpret.

While daytime and nighttime peaks can be explained quite straightforwardly through variations in temperature or available oxidants or terminators that all follow distinct diurnal trends, we also observed additional types of diurnal trends, present mostly in range 2. Factor UB2-1: Monoterpenes 1 had a peak in the morning and evening (Fig. 4), around sunrise and sunset. We can speculate that these are the periods when sunlight was still available but in limited amounts. This effect may cause an optimal situation for having both NO_3 and NO participating in the oxidation process. This is supported by the high N-atom content of the main species in this factor. Meanwhile, some other factors showed an opposite trend to UB2-1, namely minima during the morning and evening, often with a strong nighttime peak and a smaller daytime increase. Some of the most prominent factors with such behavior were SC2-3: MT monomers 2, UB2-2: MT monomers 2, UB2-3: sesquiterpene 1, and UB3-1: sesquiterpene 2. NO_3 was identified as the main oxidant for these factors based on the mass spectra and the high nighttime signals, but the local maxima around noon are surprising. Saarikoski et al. (2023) did estimate that NO_3 would have a small daytime maximum, likely due to the sinks not being fast enough to fully overwhelm the very high formation rates from high O_3 and NO_2 during this time. We cannot determine to which extent the diurnal variation in NO_3 influences these diurnal patterns. As was also the case in many situations discussed above, we are often unable to separate whether an increase is due to an enhanced source strength or a decrease in competing reaction pathways.

Comparison to previous research

HOM data from Helsinki show similarities with previous studies done on ambient HOM data in urban as well as rural environments. Yan et al. (2016) investigated HOM formation pathways at a boreal forest site (SMEAR II sta-

tion, Hyytiälä, Finland) located approximately 190 km from Helsinki and 50 km from the closest city – Tampere (with a population of approximately 250 000). A factor "Nighttype type-2", obtained from PMF analysis by Yan et al. (2016), contained MT-derived dimers formed by NO_3 and O_3 oxidation and RO_2 termination. That factor mostly consisted of $C_{20}H_{31}O_{10-18}N$ (40 %) and $C_{20}H_{32}O_{10-17}N_2$ (20 %), suggesting that the dimers detected in Hyytiälä and in Helsinki (both stations) have the same formation pathways, even though these measurement sites represent different rural and urban environments. Despite relatively similar precursors and formation pathways, far fewer similarities are found between the mass spectra of MT-derived monomer factors at these three sites. This suggests, as also mentioned above, that monomer formation pathways are much more diverse compared to dimer formation. Still, a comparison of our results with other studies done in rural environments (Massoli et al., 2018; Kürten et al., 2016) showed clearly lower resemblance between MT-derived dimers than the one described in preceding sentences, which is likely a result of different biome types in their studies (isoprene-dominated southeast USA and rural agricultural site in Germany, respectively) compared with the ones conducted in Finland.

In recent years, more research on condensable vapor formation has been conducted in urban environments heavily influenced by NO_x (Yan et al., 2022; Guo et al., 2022b; Liu et al., 2021; Nie et al., 2022; Zhang et al., 2022). Unlike in forest environments, where the fraction of nitrogen-containing HOMs is similar to the fraction of HOMs without nitrogen atoms (Yan et al., 2016; Massoli et al., 2018), condensable vapor composition in Chinese megacities is dominated by nitrogen-containing compounds, which represent approximately 60 %–85 % of all measured condensable vapors (Guo et al., 2022b; Liu et al., 2021; Nie et al., 2022; Zhang et al., 2022). This strong influence by NO_x was also observed in the present study at both stations in Helsinki. In addition, the majority of key compounds in SC1-5: nitrophenol & aliphatic are also listed as the main compounds in factors originating from aliphatic AVOCs detected in Nanjing ("Aliph-OOM") (Liu et al., 2021) and in Beijing ("aliphatic OOMs") (Guo et al., 2022b). However, depending on the time of the year, the main precursors for condensable vapors in cities in China are either AVOCs or a mix of AVOCs and BVOCs (Guo et al., 2022b; Liu et al., 2021; Nie et al., 2022). During spring, 77 % of all measured condensable vapors originate from AVOCs in Beijing (Guo et al., 2022b). This is different to Helsinki, where BVOC-derived vapors were more abundant. This dissimilarity is likely due to the AVOC : BVOC ratio being much larger in Chinese cities due to the closer proximity of much larger areas with anthropogenic emissions. In contrast, Helsinki AVOC : BVOC is much smaller due to larger BVOC emissions from abundant vegetation in the close surroundings. It is also important to notice that most studies of condensable vapors in Chinese cities (Guo et al., 2022b; Liu et al., 2021; Nie et al., 2022)

analyzed a much smaller mass range (200–400 Th or 250-400 Th), which corresponds to range 1–2 here. In our study, range 1 is the only mass range in which we find the dominant influence of anthropogenic precursors. Brean et al. (2019) also showed that MT-derived dimer concentrations were approximately 50 times lower than MT-derived monomers in Beijing, likely due to both small MT emissions and suppression of dimer formation by NO.

Implications for air quality

Ambient air pollution was recognized as the largest environmental health risk and one of the top risk factors for the loss of healthy years (Lim et al., 2012; Anderson et al., 2012; Cohen et al., 2017). Premature deaths caused by ambient air pollution are linked to particulate matter (PM) (Cohen et al., 2017; WHO, 2021), due to both short-term exposure (Pope and Dockery, 2012) and long-term exposure (Burnett et al., 2014). In many environments, including different urban areas, PM is dominated by secondary aerosol formed from condensable vapors, including HOMs. HOMs and other condensable organic vapors impact not only PM concentration but also the chemical composition of SOA and, consequently, aerosol properties like toxicity. For example, in a recent study with human alveolar epithelial cells and human monocyte cells, the organic compounds and the aging of the aerosol were major drivers of the cell-level toxicity of aerosol (Hakkarainen et al., 2022).

In this work, we found that the majority of low-volatility condensable vapors in Helsinki were impacted by both biogenic and anthropogenic precursors, despite high local anthropogenic emissions. The VOC precursors themselves were mostly of biogenic origin, i.e., BVOCs, but the oxidation process was strongly perturbed by anthropogenic activity, particularly by NO_x. While detailed similarities in mass spectra of factors were often small between the nearby sites studied here, most observed compounds at both stations were ONCs. Previous studies have shown that NO_x can change the yield of SOA formation during VOC oxidation (Mutzel et al., 2021; Jaoui et al., 2013; Ng et al., 2017), though this effect may not be as clear to observe in ambient measurements (Yan et al., 2022). In the smaller m/Q ranges studied in this work, the influence from AVOCs was larger, but we cannot deduce the impact of these factors on SOA formation due to their semi-volatile nature. Nevertheless, our results indicate that in Helsinki, and likely in other biologically influenced urban areas, anthropogenic emissions affect HOM formation and composition most strongly by the participation of NO_x in (B)VOC oxidation. That influence will be propagated to the SOA, concerning both the composition and the effective yield of SOA from the BVOC oxidation, but quantifying the ultimate impact on either of these will require further studies.

4 Conclusions

We measured the composition of condensable vapors, HOMs, during late spring at two stations separated by 900 m in different sub-environments in Helsinki, a city with considerable biogenic influence from trees. We compared HOM composition and formation pathways at the two sites, an urban background station and a street canyon, using PMF analysis to separate the complex data into co-varying compound groups. We found that the majority of the HOMs originated from BVOCs at both locations, despite them being dominated by AVOC emissions (Rantala et al., 2016; Saarikoski et al., 2023). However, we did observe a strong anthropogenic influence on the HOM formation, due to the elevated NO_x concentrations at both stations, which is consistent with previous studies conducted in urban environments (Guo et al., 2022b; Liu et al., 2021; Nie et al., 2022). The PMF factors, and their temporal behavior, were surprisingly different between the two sites, considering their relatively close proximity. Monoterpene-derived dimers were the compound groups that correlated best between the sites. On the contrary, at the street canyon site we observed a factor corresponding partly to AVOC-derived factors found in Chinese megacities (Guo et al., 2022b; Liu et al., 2021; Nie et al., 2022). The lack of a similar factor in the PMF solution from the urban background station highlights that HOM composition at two nearby sites in an urban environment can differ noticeably depending on the local anthropogenic influences. To a large extent, we expect this difference to be driven by differences in the environmental conditions, leading to distinct oxidation products even when the same VOC molecule becomes oxidized due to competition between both oxidants and RO_2 terminators.

Our work indicates that when analyzing and discussing the impact of HOMs on SOA and air quality in urban environments, we need to keep in mind the spatial inhomogeneity of urban areas in the HOM composition and formation mechanisms. Thus, a more detailed investigation of the formation and composition of HOMs in a variety of different urban sub-environments would be beneficial. Additionally, our findings are restricted to a short and biologically active period; hence follow-up research on seasonal changes is needed. Finally, we recommend that future mass spectrometric studies in urban areas employ devices with resolving power above $5000\,\mathrm{Th}\,\mathrm{Th}^{-1}$, as the mass spectra are extremely complex and thus even peak identification can be a major challenge.

Author contributions. The main ideas were formulated by OG, HT, JKo, JVN, MS, MDM TR, TP, and MK, and the results were interpreted by MOk, OG, PP, and ME. TR, HK, OG, and HT prepared the measurement methodology, and OG, MOl, JKa, HH, and HK contributed to data collection. MOk performed the data analysis, and YZ supported it. OG and ME supervised the project. HT, MDM, and TP acquired funding. MOk visualized data and prepared the manuscript with contributions from OG and ME. All the authors reviewed and commented on the manuscript.

Review statement. This paper was edited by Thomas Karl and reviewed by Yare Baker and two anonymous referees.

References

Anderson, J. O., Thundiyil, J. G., and Stolbach, A.: Clearing the Air: A Review of the Effects of Particulate Matter Air Pollution on Human Health, J. Med. Toxicol., 8, 166–175, https://doi.org/10.1007/s13181-011-0203-1, 2012.

Atkinson, R. and Arey, J.: Atmospheric degradation of volatile organic compounds, Chem. Rev., 103, 4605–4638, https://doi.org/10.1021/CR0206420, 2003.

Bianchi, F., Garmash, O., He, X., Yan, C., Iyer, S., Rosendahl, I., Xu, Z., Rissanen, M. P., Riva, M., Taipale, R., Sarnela, N., Petäjä, T., Worsnop, D. R., Kulmala, M., Ehn, M., and Junninen, H.: The role of highly oxygenated molecules (HOMs) in determining the composition of ambient ions in the boreal forest, Atmos. Chem. Phys., 17, 13819–13831, https://doi.org/10.5194/acp-17-13819-2017, 2017.

Bianchi, F., Kurtén, T., Riva, M., Mohr, C., Rissanen, M. P., Roldin, P., Berndt, T., Crounse, J. D., Wennberg, P. O., Mentel, T. F., Wildt, J., Junninen, H., Jokinen, T., Kulmala, M., Worsnop, D. R., Thornton, J. A., Donahue, N., Kjaergaard, H. G., and Ehn, M.: Highly Oxygenated Organic Molecules (HOM) from Gas-Phase Autoxidation Involving Peroxy Radicals: A Key Contributor to Atmospheric Aerosol, Chem. Rev., 119, 3472–3509, https://doi.org/10.1021/ACS.CHEMREV.8B00395, 2019.

Brean, J., Harrison, R. M., Shi, Z., Beddows, D. C. S., Acton, W. J. F., Hewitt, C. N., Squires, F. A., and Lee, J.: Observations of highly oxidized molecules and particle nucleation in the atmosphere of Beijing, Atmos. Chem. Phys., 19, 14933–14947, https://doi.org/10.5194/acp-19-14933-2019, 2019.

Burnett, R. T., Arden Pope, C., Ezzati, M., Olives, C., Lim, S. S., Mehta, S., Shin, H. H., Singh, G., Hubbell, B., Brauer, M., Ross Anderson, H., Smith, K. R., Balmes, J. R., Bruce, N. G., Kan, H., Laden, F., Prüss-Ustün, A., Turner, M. C., Gapstur, S. M., Diver, W. R., and Cohen, A.: An Integrated Risk Function for Estimating the Global Burden of Disease Attributable to Ambient Fine Particulate Matter Exposure, Environ. Health Perspect., 122, 397–403, https://doi.org/10.1289/EHP.1307049, 2014.

Canonaco, F., Crippa, M., Slowik, J. G., Baltensperger, U., and Prévôt, A. S. H.: SoFi, an IGOR-based interface for the efficient use of the generalized multilinear engine (ME-2) for the source apportionment: ME-2 application to aerosol mass spectrometer data, Atmos. Meas. Tech., 6, 3649–3661, https://doi.org/10.5194/amt-6-3649-2013, 2013.

Chen, G., Canonaco, F., Tobler, A., Aas, W., Alastuey, A., Allan, J., Atabakhsh, S., Aurela, M., Baltensperger, U., Bougiatioti, A., De Brito, J. F., Ceburnis, D., Chazeau, B., Chebaicheb, H., Daellenbach, K. R., Ehn, M., El Haddad, I., Eleftheriadis, K., Favez, O., Flentje, H., Font, A., Fossum, K., Freney, E., Gini, M., Green, D. C., Heikkinen, L., Herrmann, H., Kalogridis, A. C., Keernik, H., Lhotka, R., Lin, C., Lunder, C., Maasikmets, M., Manousakas, M. I., Marchand, N., Marin, C., Marmureanu, L., Mihalopoulos, N., Močnik, G., Nęcki, J., O'Dowd, C., Ovadnevaite, J., Peter, T., Petit, J. E., Pikridas, M., Matthew Platt, S., Pokorná, P., Poulain, L., Priestman, M., Riffault, V., Rinaldi, M., Różański, K., Schwarz, J., Sciare, J., Simon, L., Skiba, A., Slowik, J. G., Sosedova, Y., Stavroulas, I., Styszko, K., Teinemaa, E., Timonen, H., Tremper, A., Vasilescu, J., Via, M., Vodička, P., Wiedensohler, A., Zografou, O., Cruz Minguillón, M., and Prévôt, A. S. H.: European aerosol phenomenology - 8: Harmonised source apportionment of organic aerosol using 22 Year-long ACSM/AMS datasets, Environ. Int., 166, 107325, https://doi.org/10.1016/J.ENVINT.2022.107325, 2022.

Coggon, M. M., Gkatzelis, G. I., McDonald, B. C., Gilman, J. B., Schwantes, R. H., Abuhassan, N., Aikin, K. C., Arendd, M. F., Berkoff, T. A., Brown, S. S., Campos, T. L., Dickerson, R. R., Gronoff, G., Hurley, J. F., Isaacman-Vanwertz, G., Koss, A. R., Li, M., McKeen, S. A., Moshary, F., Peischl, J., Pospisilova, V., Ren, X., Wilson, A., Wu, Y., Trainer, M., and Warneke, C.: Volatile chemical product emissions enhance ozone and modulate urban chemistry, Proc. N. Acad. Sci. USA, 118, e2026653118, https://doi.org/10.1073/pnas.2026653118, 2021.

Cohen, A. J., Brauer, M., Burnett, R., Anderson, H. R., Frostad, J., Estep, K., Balakrishnan, K., Brunekreef, B., Dandona, L., Dandona, R., Feigin, V., Freedman, G., Hubbell, B., Jobling, A., Kan, H., Knibbs, L., Liu, Y., Martin, R., Morawska, L., Pope, C. A., Shin, H., Straif, K., Shaddick, G., Thomas, M., van Dingenen, R., van Donkelaar, A., Vos, T., Murray, C. J. L., and Forouzanfar, M. H.: Estimates and 25-year trends of the global burden of disease attributable to ambient air pollution: an analysis of data from the Global Burden of Diseases Study 2015, Lancet, 389, 1907–1918, https://doi.org/10.1016/S0140-6736(17)30505-6, 2017.

Crounse, J. D., Nielsen, L. B., Jørgensen, S., Kjaergaard, H. G., and Wennberg, P. O.: Autoxidation of organic compounds in the atmosphere, J. Phys. Chem. Lett., 4, 3513–3520, https://doi.org/10.1021/jz4019207, 2013.

Crutzen, P. J., Lawrence, M. G., and Pöschl, U.: On the background photochemistry of tropospheric ozone, Tellus B, 51, 123–146, https://doi.org/10.1034/J.1600-0889.1999.00010.X, 1999.

Dam, M., Draper, D. C., Marsavin, A., Fry, J. L., and Smith, J. N.: Observations of gas-phase products from the nitrate-radical-initiated oxidation of four monoterpenes, Atmos. Chem. Phys., 22, 9017–9031, https://doi.org/10.5194/acp-22-9017-2022, 2022.

Ehn, M., Thornton, J. A., Kleist, E., Sipilä, M., Junninen, H., Pullinen, I., Springer, M., Rubach, F., Tillmann, R., Lee, B., Lopez-Hilfiker, F., Andres, S., Acir, I. H., Rissanen, M., Jokinen, T., Schobesberger, S., Kangasluoma, J., Kontkanen, J., Nieminen, T., Kurtén, T., Nielsen, L. B., Jørgensen, S., Kjaergaard, H. G., Canagaratna, M., Maso, M. D., Berndt, T., Petäjä, T., Wahner, A., Kerminen, V. M., Kulmala, M., Worsnop, D. R., Wildt, J., and Mentel, T. F.: A large source of low-volatility secondary organic aerosol, Nature, 506, 476–479, https://doi.org/10.1038/nature13032, 2014.

Fry, J. L., Draper, D. C., Barsanti, K. C., Smith, J. N., Ortega, J., Winkler, P. M., Lawler, M. J., Brown, S. S., Edwards, P. M., Cohen, R. C., and Lee, L.: Secondary organic aerosol for-

mation and organic nitrate yield from NO3 oxidation of biogenic hydrocarbons, Environ. Sci. Technol., 48, 11944–11953, https://doi.org/10.1021/es502204x, 2014.

Garmash, O., Rissanen, M. P., Pullinen, I., Schmitt, S., Kausiala, O., Tillmann, R., Zhao, D., Percival, C., Bannan, T. J., Priestley, M., Hallquist, Å. M., Kleist, E., Kiendler-Scharr, A., Hallquist, M., Berndt, T., McFiggans, G., Wildt, J., Mentel, T. F., and Ehn, M.: Multi-generation OH oxidation as a source for highly oxygenated organic molecules from aromatics, Atmos. Chem. Phys., 20, 515–537, https://doi.org/10.5194/acp-20-515-2020, 2020.

Gkatzelis, G. I., Coggon, M. M., McDonald, B. C., Peischl, J., Gilman, J. B., Aikin, K. C., Robinson, M. A., Canonaco, F., Prevot, A. S. H., Trainer, M., and Warneke, C.: Observations Confirm that Volatile Chemical Products Are a Major Source of Petrochemical Emissions in U.S. Cities, Environ. Sci. Technol., 55, 4332–4343, https://doi.org/10.1021/acs.est.0c05471, 2021.

Guo, Y., Shen, H., Pullinen, I., Luo, H., Kang, S., Vereecken, L., Fuchs, H., Hallquist, M., Acir, I.-H., Tillmann, R., Rohrer, F., Wildt, J., Kiendler-Scharr, A., Wahner, A., Zhao, D., and Mentel, T. F.: Identification of highly oxygenated organic molecules and their role in aerosol formation in the reaction of limonene with nitrate radical, Atmos. Chem. Phys., 22, 11323–11346, https://doi.org/10.5194/acp-22-11323-2022, 2022a.

Guo, Y., Yan, C., Liu, Y., Qiao, X., Zheng, F., Zhang, Y., Zhou, Y., Li, C., Fan, X., Lin, Z., Feng, Z., Zhang, Y., Zheng, P., Tian, L., Nie, W., Wang, Z., Huang, D., Daellenbach, K. R., Yao, L., Dada, L., Bianchi, F., Jiang, J., Liu, Y., Kerminen, V.-M., and Kulmala, M.: Seasonal variation in oxygenated organic molecules in urban Beijing and their contribution to secondary organic aerosol, Atmos. Chem. Phys., 22, 10077–10097, https://doi.org/10.5194/acp-22-10077-2022, 2022b.

Hakkarainen, H., Salo, L., Mikkonen, S., Saarikoski, S., Aurela, M., Teinilä, K., Ihalainen, M., Martikainen, S., Marjanen, P., Lepistö, T., Kuittinen, N., Saarnio, K., Aakko-Saksa, P., Pfeiffer, T. V., Timonen, H., Rönkkö, T., and Jalava, P. I.: Black carbon toxicity dependence on particle coating: Measurements with a novel cell exposure method, Sci. Total Environ., 838, 156543, https://doi.org/10.1016/J.SCITOTENV.2022.156543, 2022.

Helin, A., Hakola, H., and Hellén, H.: Optimisation of a thermal desorption–gas chromatography–mass spectrometry method for the analysis of monoterpenes, sesquiterpenes and diterpenes, Atmos. Meas. Tech., 13, 3543–3560, https://doi.org/10.5194/amt-13-3543-2020, 2020.

Hyttinen, N., Kupiainen-Määttä, O., Rissanen, M. P., Muuronen, M., Ehn, M., and Kurtén, T.: Modeling the Charging of Highly Oxidized Cyclohexene Ozonolysis Products Using Nitrate-Based Chemical Ionization, J. Phys. Chem. A, 119, 6339–6345, https://doi.org/10.1021/acs.jpca.5b01818, 2015.

Jaoui, M., Kleindienst, T. E., Docherty, K. S., Lewandowski, M., Offenberg, J. H., Jaoui, M., Kleindienst, T. E., Docherty, K. S., Lewandowski, M., and Offenberg, J. H.: Secondary organic aerosol formation from the oxidation of a series of sesquiterpenes: α-cedrene, β-caryophyllene, α-humulene and α-farnesene with O$_3$, OH and NO$_3$ radicals, Environ. Chem., 10, 178–193, https://doi.org/10.1071/EN13025, 2013.

Järvi, L., Hannuniemi, H., Hussein, T., Junninen, H., Aalto, P. P., Hillamo, R., Mäkelä, T., Keronen, P., Siivola, E., Vesala, T., and Kulmala, M.: The urban measurement station SMEAR III: Continuous monitoring of air pollution and surface-atmosphere inter-

actions in Helsinki, Finland, Boreal Environ. Res., 14, 86–109, 2009.

Järvi, L., Kurppa, M., Kuuluvainen, H., Rönkkö, T., Karttunen, S., Balling, A., Timonen, H., Niemi, J. V., and Pirjola, L.: Determinants of spatial variability of air pollutant concentrations in a street canyon network measured using a mobile laboratory and a drone, Sci. Total Environ., 856, 158974, https://doi.org/10.1016/J.SCITOTENV.2022.158974, 2023.

Jokinen, T., Sipilä, M., Junninen, H., Ehn, M., Lönn, G., Hakala, J., Petäjä, T., Mauldin III, R. L., Kulmala, M., and Worsnop, D. R.: Atmospheric sulphuric acid and neutral cluster measurements using CI-APi-TOF, Atmos. Chem. Phys., 12, 4117–4125, https://doi.org/10.5194/acp-12-4117-2012, 2012.

Junninen, H., Lauri, A., Keronen, P., Aalto, P., Hiltunen, V., Hari, P., and Kulmala, M.: Smart-SMEAR: on-line data exploration and visualization tool for SMEAR stations, Boreal Environ. Res., 14, 447–457, 2009.

Junninen, H., Ehn, M., Petäjä, T., Luosujärvi, L., Kotiaho, T., Kostiainen, R., Rohner, U., Gonin, M., Fuhrer, K., Kulmala, M., and Worsnop, D. R.: A high-resolution mass spectrometer to measure atmospheric ion composition, Atmos. Meas. Tech., 3, 1039–1053, https://doi.org/10.5194/amt-3-1039-2010, 2010.

Kaltsonoudis, C., Kostenidou, E., Florou, K., Psichoudaki, M., and Pandis, S. N.: Temporal variability and sources of VOCs in urban areas of the eastern Mediterranean, Atmos. Chem. Phys., 16, 14825–14842, https://doi.org/10.5194/acp-16-14825-2016, 2016.

Karl, T., Striednig, M., Graus, M., Hammerle, A., and Wohlfahrt, G.: Urban flux measurements reveal a large pool of oxygenated volatile organic compound emissions, P. Natl. Acad. Sci. USA, 115, 1186–1191, https://doi.org/10.1073/pnas.1714715115, 2018.

Kaser, L., Peron, A., Graus, M., Striednig, M., Wohlfahrt, G., Juráň, S., and Karl, T.: Interannual variability of terpenoid emissions in an alpine city, Atmos. Chem. Phys., 22, 5603–5618, https://doi.org/10.5194/acp-22-5603-2022, 2022.

Kota, S. H., Park, C., Hale, M. C., Werner, N. D., Schade, G. W., and Ying, Q.: Estimation of VOC emission factors from flux measurements using a receptor model and footprint analysis, Atmos. Environ., 82, 24–35, https://doi.org/10.1016/J.ATMOSENV.2013.09.052, 2014.

Kroll, J. H. and Seinfeld, J. H.: Chemistry of secondary organic aerosol: Formation and evolution of low-volatility organics in the atmosphere, Atmos. Environ., 42, 3593–3624, https://doi.org/10.1016/J.ATMOSENV.2008.01.003, 2008.

Kürten, A., Bergen, A., Heinritzi, M., Leiminger, M., Lorenz, V., Piel, F., Simon, M., Sitals, R., Wagner, A. C., and Curtius, J.: Observation of new particle formation and measurement of sulfuric acid, ammonia, amines and highly oxidized organic molecules at a rural site in central Germany, Atmos. Chem. Phys., 16, 12793–12813, https://doi.org/10.5194/acp-16-12793-2016, 2016.

Kuuluvainen, H., Poikkimäki, M., Järvinen, A., Kuula, J., Irjala, M., Dal Maso, M., Keskinen, J., Timonen, H., Niemi, J. V., and Rönkkö, T.: Vertical profiles of lung deposited surface area concentration of particulate matter measured with a drone in a street canyon, Environ. Pollut., 241, 96–105, https://doi.org/10.1016/j.envpol.2018.04.100, 2018.

Li, X.-B., Yuan, B., Wang, S., Wang, C., Lan, J., Liu, Z., Song, Y., He, X., Huangfu, Y., Pei, C., Cheng, P., Yang, S., Qi, J.,

Wu, C., Huang, S., You, Y., Chang, M., Zheng, H., Yang, W., Wang, X., and Shao, M.: Variations and sources of volatile organic compounds (VOCs) in urban region: insights from measurements on a tall tower, Atmos. Chem. Phys., 22, 10567–10587, https://doi.org/10.5194/acp-22-10567-2022, 2022.

Lim, S. S., Vos, T., Flaxman, A. D., Danaei, G., Shibuya, K., Adair-Rohani, H., Amann, M., Anderson, H. R., Andrews, K. G., Aryee, M., Atkinson, C., Bacchus, L. J., Bahalim, A. N., Balakrishnan, K., Balmes, J., Barker-Collo, S., Baxter, A., Bell, M. L., Blore, J. D., Blyth, F., Bonner, C., Borges, G., Bourne, R., Boussinesq, M., Brauer, M., Brooks, P., Bruce, N. G., Brunekreef, B., Bryan-Hancock, C., Bucello, C., Buchbinder, R., Bull, F., Burnett, R. T., Byers, T. E., Calabria, B., Carapetis, J., Carnahan, E., Chafe, Z., Charlson, F., Chen, H., Chen, J. S., Cheng, A. T. A., Child, J. C., Cohen, A., Colson, K. E., Cowie, B. C., Darby, S., Darling, S., Davis, A., Degenhardt, L., Dentener, F., Des Jarlais, D. C., Devries, K., Dherani, M., Ding, E. L., Dorsey, E. R., Driscoll, T., Edmond, K., Ali, S. E., Engell, R. E., Erwin, P. J., Fahimi, S., Falder, G., Farzadfar, F., Ferrari, A., Finucane, M. M., Flaxman, S., Fowkes, F. G. R., Freedman, G., Freeman, M. K., Gakidou, E., Ghosh, S., Giovannucci, E., Gmel, G., Graham, K., Grainger, R., Grant, B., Gunnell, D., Gutierrez, H. R., Hall, W., Hoek, H. W., Hogan, A., Hosgood, H. D., Hoy, D., Hu, H., Hubbell, B. J., Hutchings, S. J., Ibeanusi, S. E., Jacklyn, G. L., Jasrasaria, R., Jonas, J. B., Kan, H., Kanis, J. A., Kassebaum, N., Kawakami, N., Khang, Y. H., Khatibzadeh, S., Khoo, J. P., Kok, C., Laden, F., Lalloo, R., Lan, Q., Lathlean, T., Leasher, J. L., Leigh, J., Li, Y., Lin, J. K., Lipshultz, S. E., London, S., Lozano, R., Lu, Y., Mak, J., Malekzadeh, R., Mallinger, L., Marcenes, W., March, L., Marks, R., Martin, R., McGale, P., McGrath, J., Mehta, S., Mensah, G. A., Merriman, T. R., Micha, R., Michaud, C., Mishra, V., Hanafiah, K. M., Mokdad, A. A., Morawska, L., Mozaffarian, D., Murphy, T., Naghavi, M., Neal, B., Nelson, P. K., Nolla, J. M., Norman, R., Olives, C., Omer, S. B., Orchard, J., Osborne, R., Ostro, B., Page, A., Pandey, K. D., Parry, C. D.H., Passmore, E., Patra, J., Pearce, N., Pelizzari, P. M., Petzold, M., Phillips, M. R., Pope, D., Pope, C. A., Powles, J., Rao, M., Razavi, H., Rehfuess, E. A., Rehm, J. T., Ritz, B., Rivara, F. P., Roberts, T., Robinson, C., Rodriguez-Portales, J. A., Romieu, I., Room, R., Rosenfeld, L. C., Roy, A., Rushton, L., Salomon, J. A., Sampson, U., Sanchez-Riera, L., Sanman, E., Sapkota, A., Seedat, S., Shi, P., Shield, K., Shivakoti, R., Singh, G. M., Sleet, D. A., Smith, E., Smith, K. R., Stapelberg, N. J.C., Steenland, K., Stöckl, H., Stovner, L. J., Straif, K., Straney, L., Thurston, G. D., Tran, J. H., Van Dingenen, R., Van Donkelaar, A., Veerman, J. L., Vijayakumar, L., Weintraub, R., Weissman, M. M., White, R. A., Whiteford, H., Wiersma, S. T., Wilkinson, J. D., Williams, H. C., Williams, W., Wilson, N., Woolf, A. D., Yip, P., Zielinski, J. M., Lopez, A. D., Murray, C. J. L., and Ezzati, M.: A comparative risk assessment of burden of disease and injury attributable to 67 risk factors and risk factor clusters in 21 regions, 1990–2010: A systematic analysis for the Global Burden of Disease Study 2010, Lancet, 380, 2224–2260, https://doi.org/10.1016/S0140-6736(12)61766-8, 2012.

Liu, S. C., Kley, D., McFarland, M., Mahlman, J. D., and Levy, H.: On the origin of tropospheric ozone, J. Geophys. Res., 85, 7546–7552, https://doi.org/10.1029/JC085IC12P07546, 1980.

Liu, Y., Nie, W., Li, Y., Ge, D., Liu, C., Xu, Z., Chen, L., Wang, T., Wang, L., Sun, P., Qi, X., Wang, J., Xu, Z., Yuan, J., Yan, C., Zhang, Y., Huang, D., Wang, Z., Donahue, N. M., Worsnop, D., Chi, X., Ehn, M., and Ding, A.: Formation of condensable organic vapors from anthropogenic and biogenic volatile organic compounds (VOCs) is strongly perturbed by NO_x in eastern China, Atmos. Chem. Phys., 21, 14789–14814, https://doi.org/10.5194/acp-21-14789-2021, 2021.

Massoli, P., Stark, H., Canagaratna, M. R., Krechmer, J. E., Xu, L., Ng, N. L., Mauldin, R. L., Yan, C., Kimmel, J., Misztal, P. K., Jimenez, J. L., Jayne, J. T., and Worsnop, D. R.: Ambient Measurements of Highly Oxidized Gas-Phase Molecules during the Southern Oxidant and Aerosol Study (SOAS) 2013, ACS Earth Sp. Chem., 2, 653–672, https://doi.org/10.1021/acsearthspacechem.8b00028, 2018.

McDonald, B. C., De Gouw, J. A., Gilman, J. B., Jathar, S. H., Akherati, A., Cappa, C. D., Jimenez, J. L., Lee-Taylor, J., Hayes, P. L., McKeen, S. A., Cui, Y. Y., Kim, S. W., Gentner, D. R., Isaacman-VanWertz, G., Goldstein, A. H., Harley, R. A., Frost, G. J., Roberts, J. M., Ryerson, T. B., and Trainer, M.: Volatile chemical products emerging as largest petrochemical source of urban organic emissions, Science, 359, 760–764, https://doi.org/10.1126/science.aaq0524, 2018.

Molteni, U., Bianchi, F., Klein, F., El Haddad, I., Frege, C., Rossi, M. J., Dommen, J., and Baltensperger, U.: Formation of highly oxygenated organic molecules from aromatic compounds, Atmos. Chem. Phys., 18, 1909–1921, https://doi.org/10.5194/acp-18-1909-2018, 2018.

Mutzel, A., Zhang, Y., Böge, O., Rodigast, M., Kolodziejczyk, A., Wang, X., and Herrmann, H.: Importance of secondary organic aerosol formation of α-pinene, limonene, and m-cresol comparing day- and nighttime radical chemistry, Atmos. Chem. Phys., 21, 8479–8498, https://doi.org/10.5194/acp-21-8479-2021, 2021.

Ng, N. L., Herndon, S. C., Trimborn, A., Canagaratna, M. R., Croteau, P. L., Onasch, T. B., Sueper, D., Worsnop, D. R., Zhang, Q., Sun, Y. L., and Jayne, J. T.: An Aerosol Chemical Speciation Monitor (ACSM) for Routine Monitoring of the Composition and Mass Concentrations of Ambient Aerosol, Aerosol Sci. Technol., 45, 780–794, https://doi.org/10.1080/02786826.2011.560211, 2011.

Ng, N. L., Brown, S. S., Archibald, A. T., Atlas, E., Cohen, R. C., Crowley, J. N., Day, D. A., Donahue, N. M., Fry, J. L., Fuchs, H., Griffin, R. J., Guzman, M. I., Herrmann, H., Hodzic, A., Iinuma, Y., Jimenez, J. L., Kiendler-Scharr, A., Lee, B. H., Luecken, D. J., Mao, J., McLaren, R., Mutzel, A., Osthoff, H. D., Ouyang, B., Picquet-Varrault, B., Platt, U., Pye, H. O. T., Rudich, Y., Schwantes, R. H., Shiraiwa, M., Stutz, J., Thornton, J. A., Tilgner, A., Williams, B. J., and Zaveri, R. A.: Nitrate radicals and biogenic volatile organic compounds: oxidation, mechanisms, and organic aerosol, Atmos. Chem. Phys., 17, 2103–2162, https://doi.org/10.5194/acp-17-2103-2017, 2017.

Nie, W., Yan, C., Huang, D. D., Wang, Z., Liu, Y., Qiao, X., Guo, Y., Tian, L., Zheng, P., Xu, Z., Li, Y., Xu, Z., Qi, X., Sun, P., Wang, J., Zheng, F., Li, X., Yin, R., Dallenbach, K. R., Bianchi, F., Petäjä, T., Zhang, Y., Wang, M., Schervish, M., Wang, S., Qiao, L., Wang, Q., Zhou, M., Wang, H., Yu, C., Yao, D., Guo, H., Ye, P., Lee, S., Li, Y. J., Liu, Y., Chi, X., Kerminen, V.-M., Ehn, M., Donahue, N. M., Wang, T., Huang, C., Kulmala, M., Worsnop, D., Jiang, J., and Ding, A.: Secondary organic aerosol formed by condensing anthropogenic vapours over China's megacities,

Nat. Geosci., 15, 255–261, https://doi.org/10.1038/s41561-022-00922-5, 2022.

Nie, W., Yan, C., Yang, L., Roldin, P., Liu, Y., Vogel, A. L., Molteni, U., Stolzenburg, D., Finkenzeller, H., Amorim, A., Bianchi, F., Curtius, J., Dada, L., Draper, D. C., Duplissy, J., Hansel, A., He, X. C., Hofbauer, V., Jokinen, T., Kim, C., Lehtipalo, K., Nichman, L., Mauldin, R. L., Makhmutov, V., Mentler, B., Mizelli-Ojdanic, A., Petäjä, T., Quéléver, L. L. J., Schallhart, S., Simon, M., Tauber, C., Tomé, A., Volkamer, R., Wagner, A. C., Wagner, R., Wang, M., Ye, P., Li, H., Huang, W., Qi, X., Lou, S., Liu, T., Chi, X., Dommen, J., Baltensperger, U., El Haddad, I., Kirkby, J., Worsnop, D., Kulmala, M., Donahue, N. M., Ehn, M., and Ding, A.: NO at low concentration can enhance the formation of highly oxygenated biogenic molecules in the atmosphere, Nat. Commun., 141, 1–11, https://doi.org/10.1038/s41467-023-39066-4, 2023.

Okuljar, M.: Measurement report: The influence of traffic and new particle formation on the size distribution of 1–800 nm particles in Helsinki: a street canyon and an urban background station comparison, Zenodo [data set], https://doi.org/10.5281/zenodo.4884875, 2021.

Okuljar, M., Kuuluvainen, H., Kontkanen, J., Garmash, O., Olin, M., Niemi, J. V., Timonen, H., Kangasluoma, J., Tham, Y. J., Baalbaki, R., Sipilä, M., Salo, L., Lintusaari, H., Portin, H., Teinilä, K., Aurela, M., Dal Maso, M., Rönkkö, T., Petäjä, T., and Paasonen, P.: Measurement report: The influence of traffic and new particle formation on the size distribution of 1–800 nm particles in Helsinki – a street canyon and an urban background station comparison, Atmos. Chem. Phys., 21, 9931–9953, https://doi.org/10.5194/acp-21-9931-2021, 2021.

Okuljar, M., Garmash, O., Olin, M., Kalliokoski, J., Timonen, H., Niemi, J. V., Paasonen, P., Kontkanen, J., Zhang, Y., Hellén, H., Kuuluvainen, H., Aurela, M., Manninen, H. E., Sipilä, M., Rönkkö, T., Petäjä, T., Kulmala, M., Dal Maso, M., and Ehn, M.: Dataset from "Influence of anthropogenic emissions on the composition of highly oxygenated organic molecules in Helsinki: a street canyon and urban background station comparison", Zenodo [data set], https://doi.org/10.5281/zenodo.8273030, 2023.

Olin, M., Kuuluvainen, H., Aurela, M., Kalliokoski, J., Kuittinen, N., Isotalo, M., Timonen, H. J., Niemi, J. V., Rönkkö, T., and Dal Maso, M.: Traffic-originated nanocluster emission exceeds H_2SO_4-driven photochemical new particle formation in an urban area, Atmos. Chem. Phys., 20, 1–13, https://doi.org/10.5194/acp-20-1-2020, 2020.

Paatero, P.: Least squares formulation of robust non-negative factor analysis, Chemom. Intell. Lab. Syst., 37, 23–35, https://doi.org/10.1016/S0169-7439(96)00044-5, 1997.

Paatero, P.: The Multilinear Engine – A Table-Driven, Least Squares Program for Solving Multilinear Problems, Including the n-Way Parallel Factor Analysis Model, 8, 854–888, https://doi.org/10.1080/10618600.1999.10474853, 1999.

Paatero, P. and Hopke, P. K.: Discarding or downweighting high-noise variables in factor analytic models, Anal. Chim. Acta, 490, 277–289, https://doi.org/10.1016/S0003-2670(02)01643-4, 2003.

Paatero, P. and Tapper, U.: Positive matrix factorization: A non-negative factor model with optimal utilization of error estimates of data values, Environmetrics, 5, 111–126, https://doi.org/10.1002/ENV.3170050203, 1994.

Pandis, S. N., Harley, R. A., Cass, G. R., and Seinfeld, J. H.: Secondary organic aerosol formation and transport, Atmos. Environ. A, 26, 2269–2282, https://doi.org/10.1016/0960-1686(92)90358-R, 1992.

Peräkylä, O., Riva, M., Heikkinen, L., Quéléver, L., Roldin, P., and Ehn, M.: Experimental investigation into the volatilities of highly oxygenated organic molecules (HOMs), Atmos. Chem. Phys., 20, 649–669, https://doi.org/10.5194/acp-20-649-2020, 2020.

Pope, C. A. and Dockery, D. W.: Health Effects of Fine Particulate Air Pollution: Lines that Connect, J. Air Waste Manag. Assoc., 56, 709–742, https://doi.org/10.1080/10473289.2006.10464485, 2012.

Pullinen, I., Schmitt, S., Kang, S., Sarrafzadeh, M., Schlag, P., Andres, S., Kleist, E., Mentel, T. F., Rohrer, F., Springer, M., Tillmann, R., Wildt, J., Wu, C., Zhao, D., Wahner, A., and Kiendler-Scharr, A.: Impact of NO_x on secondary organic aerosol (SOA) formation from α-pinene and β-pinene photooxidation: the role of highly oxygenated organic nitrates, Atmos. Chem. Phys., 20, 10125–10147, https://doi.org/10.5194/acp-20-10125-2020, 2020.

Quéléver, L. L. J., Kristensen, K., Normann Jensen, L., Rosati, B., Teiwes, R., Daellenbach, K. R., Peräkylä, O., Roldin, P., Bossi, R., Pedersen, H. B., Glasius, M., Bilde, M., and Ehn, M.: Effect of temperature on the formation of highly oxygenated organic molecules (HOMs) from alpha-pinene ozonolysis, Atmos. Chem. Phys., 19, 7609–7625, https://doi.org/10.5194/acp-19-7609-2019, 2019.

Rantala, P., Järvi, L., Taipale, R., Laurila, T. K., Patokoski, J., Kajos, M. K., Kurppa, M., Haapanala, S., Siivola, E., Petäjä, T., Ruuskanen, T. M., and Rinne, J.: Anthropogenic and biogenic influence on VOC fluxes at an urban background site in Helsinki, Finland, Atmos. Chem. Phys., 16, 7981–8007, https://doi.org/10.5194/acp-16-7981-2016, 2016.

Reimann, S. and Lewis, A. C.: Anthropogenic VOCs, in: Volatile Organic Compounds in the Atmosphere, edited by: Koppmann, R., Blackwell Publishing Ltd, https://doi.org/10.1002/9780470988657, 2007.

Richters, S., Herrmann, H., and Berndt, T.: Highly Oxidized RO2 Radicals and Consecutive Products from the Ozonolysis of Three Sesquiterpenes, Environ. Sci. Technol., 50, 2354–2362, https://doi.org/10.1021/acs.est.5b05321, 2016.

Saarikoski, S., Hellén, H., Praplan, A. P., Schallhart, S., Clusius, P., Niemi, J. V., Kousa, A., Tykkä, T., Kouznetsov, R., Aurela, M., Salo, L., Rönkkö, T., Barreira, L. M. F., Pirjola, L., and Timonen, H.: Characterization of volatile organic compounds and submicron organic aerosol in a traffic environment, Atmos. Chem. Phys., 23, 2963–2982, https://doi.org/10.5194/acp-23-2963-2023, 2023.

Seinfeld, J. H. and Pandis, S. N.: Atmospheric Chemistry and Physics: From Air Pollution to Climate Change, Third edit., Hoboken, New Jersey, John Wiley & Sons, Inc., ISBN 978-1-118-94740-1, 2016.

Shen, H., Zhao, D., Pullinen, I., Kang, S., Vereecken, L., Fuchs, H., Acir, I. H., Tillmann, R., Rohrer, F., Wildt, J., Kiendler-Scharr, A., Wahner, A., and Mentel, T. F.: Highly Oxygenated Organic Nitrates Formed from NO3Radical-Initiated Oxidation of β-Pinene, Environ. Sci. Technol., 55, 15658–15671, https://doi.org/10.1021/acs.est.1c03978, 2021.

SmartSMEAR: https://smear.avaa.csc.fi/, AVAA [data set], last access: 22 August 2023.

Timonen, H., Karjalainen, P., Saukko, E., Saarikoski, S., Aakko-Saksa, P., Simonen, P., Murtonen, T., Dal Maso, M., Kuuluvainen, H., Bloss, M., Ahlberg, E., Svenningsson, B., Pagels, J., Brune, W. H., Keskinen, J., Worsnop, D. R., Hillamo, R., and Rönkkö, T.: Influence of fuel ethanol content on primary emissions and secondary aerosol formation potential for a modern flex-fuel gasoline vehicle, Atmos. Chem. Phys., 17, 5311–5329, https://doi.org/10.5194/acp-17-5311-2017, 2017.

Valiev, R. R., Hasan, G., Salo, V. T., Kubeèka, J., and Kurten, T.: Intersystem Crossings Drive Atmospheric Gas-Phase Dimer Formation, J. Phys. Chem. A, 123, 6596–6604, https://doi.org/10.1021/acs.jpca.9b02559, 2019.

Wang, Z., Ehn, M., Rissanen, M. P., Garmash, O., Quéléver, L., Xing, L., Monge-Palacios, M., Rantala, P., Donahue, N. M., Berndt, T., and Sarathy, S. M.: Efficient alkane oxidation under combustion engine and atmospheric conditions, Commun. Chem. 2021 41, 1–8, https://doi.org/10.1038/s42004-020-00445-3, 2021.

Watson, J. G., Chow, J. C., and Fujita, E. M.: Review of volatile organic compound source apportionment by chemical mass balance, Atmos. Environ., 35, 1567–1584, https://doi.org/10.1016/S1352-2310(00)00461-1, 2001.

Wayne, R. P.: Chemistry of atmospheres: an introduction to the chemistry of the atmospheres of earth, the planets, and their satellites, 3rd ed., Oxford, Oxford University Press, ISBN 978-0-19-850375-0, 2000.

Wayne, R. P., Barnes, I., Biggs, P., Burrows, J. P., Canosa-Mas, C. E., Hjorth, J., Le Bras, G., Moortgat, G. K., Perner, D., Poulet, G., Restelli, G., and Sidebottom, H.: The nitrate radical: Physics, chemistry, and the atmosphere, Atmos. Environ. A, 25, 1–203, https://doi.org/10.1016/0960-1686(91)90192-A, 1991.

WHO: WHO global air quality guidelines: particulate matter (PM2.5 and PM10), ozone, nitrogen dioxide, sulfur dioxide and carbon monoxide, https://apps.who.int/iris/handle/10665/345329 (last access: 30 August 2023), 2021.

Yan, C., Nie, W., Äijälä, M., Rissanen, M. P., Canagaratna, M. R., Massoli, P., Junninen, H., Jokinen, T., Sarnela, N., Häme, S. A. K., Schobesberger, S., Canonaco, F., Yao, L., Prévôt, A. S. H., Petäjä, T., Kulmala, M., Sipilä, M., Worsnop, D. R., and Ehn, M.: Source characterization of highly oxidized multifunctional compounds in a boreal forest environment using positive matrix factorization, Atmos. Chem. Phys., 16, 12715–12731, https://doi.org/10.5194/acp-16-12715-2016, 2016.

Yan, C., Nie, W., Vogel, A. L., Dada, L., Lehtipalo, K., Stolzenburg, D., Wagner, R., Rissanen, M. P., Xiao, M., Ahonen, L., Fischer, L., Rose, C., Bianchi, F., Gordon, H., Simon, M., Heinritzi, M., Garmash, O., Roldin, P., Dias, A., Ye, P., Hofbauer, V., Amorim, A., Bauer, P. S., Bergen, A., Bernhammer, A. K., Breitenlechner, M., Brilke, S., Buchholz, A., Mazon, S. B., Canagaratna, M. R., Chen, X., Ding, A., Dommen, J., Draper, D. C., Duplissy, J., Frege, C., Heyn, C., Guida, R., Hakala, J., Heikkinen, L., Hoyle, C. R., Jokinen, T., Kangasluoma, J., Kirkby, J., Kontkanen, J., Kürten, A., Lawler, M. J., Mai, H., Mathot, S., Mauldin, R. L., Molteni, U., Nichman, L., Nieminen, T., Nowak, J., Ojdanic, A., Onnela, A., Pajunoja, A., Petäjä, T., Piel, F., Quéléver, L. L. J., Sarnela, N., Schallhart, S., Sengupta, K., Sipilä, M., Tomé, A., Tröstl, J., Väisänen, O., Wagner, A. C., Ylisirniö, A., Zha,

Q., Baltensperger, U., Carslaw, K. S., Curtius, J., Flagan, R. C., Hansel, A., Riipinen, I., Smith, J. N., Virtanen, A., Winkler, P. M., Donahue, N. M., Kerminen, V. M., Kulmala, M., Ehn, M., and Worsnop, D. R.: Size-dependent influence of nox on the growth rates of organic aerosol particles, Sci. Adv., 6, 4945–4972, https://doi.org/10.1126/sciadv.aay4945, 2020.

Yan, C., Shen, Y., Stolzenburg, D., Dada, L., Qi, X., Hakala, S., Sundström, A.-M., Guo, Y., Lipponen, A., Kokkonen, T. V., Kontkanen, J., Cai, R., Cai, J., Chan, T., Chen, L., Chu, B., Deng, C., Du, W., Fan, X., He, X.-C., Kangasluoma, J., Kujansuu, J., Kurppa, M., Li, C., Li, Y., Lin, Z., Liu, Y., Liu, Y., Lu, Y., Nie, W., Pulliainen, J., Qiao, X., Wang, Y., Wen, Y., Wu, Y., Yang, G., Yao, L., Yin, R., Zhang, G., Zhang, S., Zheng, F., Zhou, Y., Arola, A., Tamminen, J., Paasonen, P., Sun, Y., Wang, L., Donahue, N. M., Liu, Y., Bianchi, F., Daellenbach, K. R., Worsnop, D. R., Kerminen, V.-M., Petäjä, T., Ding, A., Jiang, J., and Kulmala, M.: The effect of COVID-19 restrictions on atmospheric new particle formation in Beijing, Atmos. Chem. Phys., 22, 12207–12220, https://doi.org/10.5194/acp-22-12207-2022, 2022.

Zha, Q., Yan, C., Junninen, H., Riva, M., Sarnela, N., Aalto, J., Quéléver, L., Schallhart, S., Dada, L., Heikkinen, L., Peräkylä, O., Zou, J., Rose, C., Wang, Y., Mammarella, I., Katul, G., Vesala, T., Worsnop, D. R., Kulmala, M., Petäjä, T., Bianchi, F., and Ehn, M.: Vertical characterization of highly oxygenated molecules (HOMs) below and above a boreal forest canopy, Atmos. Chem. Phys., 18, 17437–17450, https://doi.org/10.5194/acp-18-17437-2018, 2018.

Zhang, Q., Jimenez, J. L., Canagaratna, M. R., Ulbrich, I. M., Ng, N. L., Worsnop, D. R., and Sun, Y.: Understanding atmospheric organic aerosols via factor analysis of aerosol mass spectrometry: A review, Anal. Bioanal. Chem., 401, 3045–3067, https://doi.org/10.1007/s00216-011-5355-y, 2011.

Zhang, Y., Peräkylä, O., Yan, C., Heikkinen, L., Äijälä, M., Daellenbach, K. R., Zha, Q., Riva, M., Garmash, O., Junninen, H., Paatero, P., Worsnop, D., and Ehn, M.: A novel approach for simple statistical analysis of high-resolution mass spectra, Atmos. Meas. Tech., 12, 3761–3776, https://doi.org/10.5194/amt-12-3761-2019, 2019.

Zhang, Y., Peräkylä, O., Yan, C., Heikkinen, L., Äijälä, M., Daellenbach, K. R., Zha, Q., Riva, M., Garmash, O., Junninen, H., Paatero, P., Worsnop, D., and Ehn, M.: Insights into atmospheric oxidation processes by performing factor analyses on subranges of mass spectra, Atmos. Chem. Phys., 20, 5945–5961, https://doi.org/10.5194/acp-20-5945-2020, 2020.

Zhang, Y., Li, D., Ma, Y., Dubois, C., Wang, X., Perrier, S., Chen, H., Wang, H., Jing, S., Lu, Y., Lou, S., Yan, C., Nie, W., Chen, J., Huang, C., George, C., and Riva, M.: Field Detection of Highly Oxygenated Organic Molecules in Shanghai by Chemical Ionization-Orbitrap, Environ. Sci. Technol., 56, 7608–7617, https://doi.org/10.1021/acs.est.1c08346, 2022.